ABSTRACT

Title of Document: STABILIZATION OF RECYCLED BASE MATERIALS WITH HIGH CARBON FLY ASH

Bora Cetin, Master of Science, 2009

Directed By: Associate Professor, Ahmet H. Aydilek, Civil and Environmental Engineering Department

A study was conducted to stabilize low stiffness road surface material with high carbon fly ash. The non-cementitious Maryland fly ash was activated with another recycled material, lime kiln dust (LKD). California bearing ratio (CBR) and resilient modulus tests were conducted to determine the strength and stiffness, respectively, of the stabilized materials. Addition of LKD and curing of specimens generally increased CBR and summary resilient modulus (SM_R) and lowered plastic strains, whereas fly ash addition alone decreased the strength and stiffness due to the non-cementitious nature of the ash. CBR increased with increasing CaO content as well as with CaO/SiO_2 and $CaO/(SiO_2 + Al_2O_3)$ ratio of the mixtures; however, these parameters could not be correlated with the SM_R. The unpaved road materials stabilized with LKD and fly ash is expected to lose 31 to 67% of their initial moduli after twelve cycles of freezing and thawing. Finally, required base thicknesses were calculated using the laboratory-based strength parameters.

STABILIZATION OF RECYLED BASE MATERIALS WITH HIGH CARBON FLY ASH

By

Bora Cetin

Thesis submitted to the Faculty of the Graduate School of the
University of Maryland, College Park, in partial fulfillment
of the requirements for the degree of
Master of Science
2009

Advisory Committee:
Associate Professor Dr. Ahmet H. Aydilek, Advisor
Professor Dr. Sherif M. Aggour, Committee Member
Professor Dr. Deborah J. Goodings, Committee Member

ACKNOWLEDGEMENT

First and foremost, I would like to thank my advisor, Professor Ahmet H. Aydilek, for his enthusiasm and guidance throughout my graduate studies at the University of Maryland – College Park. Thanks also to Professors Deborah J. Goodings and M. Sherif Aggour for being part of my committee. I also would like to thank Professor Yucel Guney for his effort in microscopy analysis of cured specimens. Thanks to Maryland State Highway Administration to help us to run resilient modulus test and provide us necessary information's about highway construction that are used in State of Maryland.

TABLE OF CONTENTS

ACKNOWLEDGEMENT ii
TABLE OF CONTENTS iii
LIST OF TABLES iv
LIST OF FIGURES v
1. INTRODUCTION 1
2. MATERIALS 6
3. METHODS 8
3.1 CALIFORNIA BEARING RATIO TEST 8
3.2 RESILIENT MODULUS TEST 9
3.3 MICROSCOPY ANALYSIS 11
4. RESULTS AND ANALYSIS 12
4.1 RESULTS OF CALIFORNIA BEARING RATIO 12
4.2 RESULTS OF RESILIENT MODULUS TEST 15
5.2.1 Effects of Curing Time, LKD addition on Summary Resilient Moduli and Plastic Strain 15
5.2.2 Effect of Freeze – Thaw on Summary Resilient Moduli 19
5. PRACTICAL IMPLICATIONS 21
5.1 HIGHWAY BASE DESIGN 21
5.2 COST CALCULATIONS 23
6. CONCLUSIONS 25
REFERENCES 27
TABLES 33
FIGURES 42
APPENDIX A 59
APPENDIX B 62
APPENDIX C 70
APPENDIX D 73
APPENDIX E 76

LIST OF TABLES

TABLE 1 a. Index properties of the materials used in the current study.

TABLE 1 b. Chemical compostion of the fly ashes. Concentrations of major minerals determined by X – ray fluorences spectroscopy analysis.

TABLE 2. Legend and compositions of the mixtures.

TABLE 3. Power model fitting parameters and measured plastic strains for resilient modulus tests.

TABLE 4. CBR and summary resilient modulus values.

TABLE 5. Chemical compositons of mixtures prepared with three different fly ashes.

TABLE 6. Effect of freezing and thawing cycles on summary resilient moduli..

TABLE 7. Required base thickness for different mixture designs for two traffic conditions under excellent drainage condition.

TABLE 8. Cost analysis for different mixture designs for two different traffic conditions under excellent drainage condition.

TABLE A.1. Properties of Maryland fly ashes with ASTM C 618 chemical and physical criteria for class C and class F fly ash.

TABLE B.1. AASHTO 307 – 99 resilient modulus testing sequence for base and subbase materials.

TABLE C.1. Predicted SM_R values based on CBR values.

TABLE D.1. Base thickness values based on SM_R values for traffic case I

TABLE D.2. Base thickness values based on SM_R values for traffic case II

TABLE E.1. Required base thickness for different mixture designs for two different traffic conditions under good drainage condition.

TABLE E.2. Required base thickness for different mixture designs for two different traffic conditions under fair drainage condition.

TABLE E.3. Required base thickness for different mixture designs for two different traffic conditions under poor drainage condition.

TABLE E.4.Cost analysis for different mixture designs for two different traffic conditions under good drainage condition.

TABLE E.5.Cost analysis for different mixture designs for two different traffic conditions under fair drainage condition.

TABLE E.6.Cost analysis for different mixture designs for two different traffic conditions under poor drainage condition.

LIST OF FIGURES

FIGURE 1. Comparison of unpaved road material and the two materials used in base construction in Maryland to (a) VDOT base materials specification, and (b) AASHTO specification.

FIGURE 2. Effect of curing time on CBR of mixtures prepared with (a) Brandon Shores fly ash, (b) Paul Smith fly ash, (c) Dickerson Precipitator fly ash.

FIGURE 3. SEM photograph of (a) Brandon Shores fly ash, (b) unpaved road material amended with 10% Brandon Shores fly ash and 2.5% LKD by weight, (c) Dickerson precipitator fly ash, and (d) unpaved road material amended with 20% Dickerson Precipitator fly ash and 5% LKD by weight.

FIGURE 4. EDX plot of the SEM photograph of (a) Dickerson Precipitator fly ash, and (b) 7-day cured unpaved road material amended with 20% Dickerson Precipitator fly ash and 5% LKD by weight.

FIGURE 5. Effect of LKD contents on (a) CBR and (b) SM_R of 28-day cured specimens.

FIGURE 6. Effect of CaO content, (b) CaO/SiO_2, (c) $CaO/(SiO_2 + Al_2O_3)$, and fineness on CBR.

FIGURE 7. Effect of (a) Silica ratio, (b) alumina ratio, (c) lime saturation factor, and (fly ash percentage on CBR.

FIGURE 8. CBR versus measured and predicted SM_R for (a) 1 day cured specimens, and (b) 7 days cured specimens.

FIGURE 9. Effect of curing time on SM_R of mixtures prepared with (a) Brandon Shores fly ash, (b) Paul Smith fly ash, and (c) Dickerson Precipitator fly ash.

FIGURE 10. Resilient Modulus of the 28-daycured specimens with varying bulk stresses: Mixtures prepared with (a) Paul Smith fly ash, and (b) Dickerson Precipitator fly ash.

FIGURE 11. Effect of CaO content, (b) CaO/SiO2, (c) CaO/(SiO2 + Al2O3), and fineness on SM_R.

FIGURE 12. Effect of (a) Silica ratio, (b) alumina ratio, (c) lime saturation factor, and (d) fly ash percentage on SM_R.

FIGURE 13. Effect of freeze and thaw cycles on SM_R values.

FIGURE 14. Effect of freeze and thaw cycles on water contents.

FIGURE 15. Summary resilient modulus as a function of base layer thickness.

FIGURE B.1.Compaction curves for (a) conventional base materials, (b) mixtures prepared with Brandon Shores fly ash, (c) mixtures prepared with Paul Smith fly ash, and (d) mixtures prepared with Dickerson Precipitator fly ash.

FIGURE B.2. Photo of Resilient Modulus Testing Equipment.

FIGURE B.3. GAB (a), URM (b), and BRG (c) .

FIGURE C.1. CBR versus measured SM_R vs. CBR graph for (a) 1 day cured specimens, and (b) 7 days cured specimens.

FIGURE D.1. Required thickness vs. number of freeze and thaw cycles (a) traffic case I, and traffic case II.

FIGURE E.1. Effect of LKD addition (a), (b), (c) and traffic conditions (d), (e), (f) on total construction fee of the highway base layer.

1. INTRODUCTION

American Society of Civil Engineers estimates that $2.2 trillion is needed over a five-year period to bring the nation's infrastructure to a good condition. Establishing a long-term development and maintenance plan is a national priority. Large volumes of earthen materials are used in construction each year in the United States. In many cases, these materials can be replaced with reclaimed highway paving materials, secondary materials, suitable waste materials and construction debris that are normally disposed in landfills, and can generate millions of dollars savings to taxpayers. Reuse in construction has several benefits, including reduction in solid waste disposal costs incurred by industry, reduction in landfill requirements, minimization of damage to natural resources caused by excavating earthen materials for construction, obtaining added value from waste materials, conservation of production energy, and ultimately providing sustainable construction and economic growth.

Legislations have been promulgated in many states that remove barriers to large-scale beneficial reuse of recycled materials, to reduce construction costs and increase sustainability. As a result, there is a policy shift, both nationally and at the state level, aimed at substantially increasing the use of such materials in geotechnical construction. For instance, one material that has been increasingly dealt with is road surface material from an unpaved road or a road undergoing rehabilitation and uses it as the base layer for newly paved roads (Hatipoglu et al. 2008). Due to its low strength and stiffness, the material often has to be stabilized by adding good quality granular material, or by blending with hydrated lime and fly ash.

Over 60% of the electricity generated in the United States is produced by coal combustion, with resulting abundant quantities of fly ash as residue, which presents another environmental challenge. Fly ash has been used as bulk fill material in geotechnical fill, such as in construction of embankments, dikes, and road subgrade (DiGioia and Nuzzo 1972, Gray and Lin 1972). The advantages of using fly ash as a bulk fill material include low cost, low unit weight, and good strength. In Eastern parts of the United States, anthracite and bituminous coals are burned by the power plants and, as a result, non-cementitious ashes (Class F or off-spec fly ashes) are produced. These fly ashes contain high amounts of SiO_2 and Al_2O_3, which can react with an activator rich in CaO (e.g., lime, cement, lime or cement kiln dust) in the presence of moisture to form cementitious compounds for stabilization applications where additional strength gain is needed (e.g., base stabilization).

Fly ash is generally reused in concrete production. However, the fly ashes produced by several power plants in United States occasionally contains significant amounts of unburned carbon (i.e., high loss on ignition) due to the increasingly common use of low nitrogen oxide (NO_x) and sulphur oxide (SO_x) burners in recent years. This ash has a carbon content of 12-25%, cannot be efficiently re-burnt by using current technology, and has no value as a concrete additive as the unburned carbon tends to adsorb the air entrainment admixtures that are added to the cement to prevent crack formation and propagation. These ashes are typically classified as off-spec fly ashes meaning that they do not meet the physical and chemical requirements criteria outlined in ASTM C 618. Recent data indicate that approximately 68% of this high-carbon fly ash (HCFA) is placed in landfills, thereby consuming valuable land space and creating the

potential to impact terrestrial and aquatic resources in Maryland. Roadways have high potential for large volume use of HCFA. HCFA can be activated with lime kiln dust (a disposed residue of lime production plants) and used as the base layer for newly paved roads.

Significant efforts have been made to use fly ashes in stabilization of highways base structures, unpaved roads and soil stabilization. Arora and Aydilek (2005) evaluated the engineering properties of Class F fly ash amended soils as highway base materials. Cement-activated fly ash increased the California bearing ratio (CBR), unconfined compression strength, and resilient modulus (M_r) of sandy soils with plastic fines contents ranging from 18 to 30%. Similar observations were made Vishwanathan et al. (1997) when silty and sandy soils were stabilized with lime-activated-Class F fly ash for their possible use in highway bases. Hatipoglu et al. (2008) showed through unconfined compression, CBR and resilient modulus tests that self-cementitious Class C fly ash can be a viable binder for stabilization of recycled asphalt pavement material (RPM) for base applications. Li et al. (2007) conducted laboratory tests to evaluate the use of RPM blended with fly ash as base course. CBR of RPM increased from 3-17 to 70-94 with the addition of fly ash. Similarly, addition of fly ash caused more than two-fold increase in M_r of laboratory RPM specimens. Camargo (2008) showed that addition of 10-15% by weight of Class C fly ash increases the CBR and resilient modulus of recycled pavement material (RPM) and road surface gravel by 3 to 6 and 9 to 22 times, respectively. Camargo (2008) has also observed a 6 to 11 and 34 to 57 times increase in CBR and resilient modulus of road surface gravel when stabilized with 10 and 15% Class C fly ash, respectively. In a study conducted by Wen et al. (2007, 2008) high carbon self-

cementitious fly ash was shown to increase the strength and stiffness of RPM. CBR and M_r of fly ash-stabilized RPM were higher than CBR and M_r for RPM without fly ash; both engineering properties were comparable to the CBR of conventional crushed aggregate. The plastic deformations for RPM were generally decreased by addition of fly ash.

Previous research has shown that self-cementing fly ash can be an effective binder for stabilizing soils for highway bases (Consoli et al. 2001, Zaman et al. 2003, Arora and Aydilek 2005, Edil et al. 2006, Kumar et al. 2007, Buhler and Cerato 2007, Hatipoglu et al. 2008, Saylak et al.2008, Shao et al. 2008, Wen et al. 2008, Camargo et al. 2008). However, limited information exists on the reuse of high carbon off-spec fly ash in construction of highway pavements. This is particularly important when high carbon fly ash is non-cementitious (e.g., Maryland fly ashes) and calcium-rich activators are required to generate pozzolanic reactions. Thus, there is a need to evaluate the strength and stiffness of base layers stabilized with high carbon fly ash. To respond to this need, a battery of tests was conducted on unpaved road surface material-fly ash mixtures amended with lime kiln dust for its possible use in highway base construction. California bearing ratio (CBR) and resilient modulus (M_R) as well as scanning electron microscopy (SEM) analyses were conducted to investigate the engineering properties of granular soil-fly ash mixtures with and without lime kiln dust (LKD), and to study the effect of curing time on soil-fly ash-LKD mixtures. The effect of winter conditions were also evaluated by performing resilient modulus tests on the specimens after a series of freeze-thaw cycles.

Another issue that impedes soil stabilization with fly ash is the potential for groundwater and other environmental impacts caused by metals in the fly ash. Fly ash contains a small amount of trace metals that can have environmental consequences when fly ash is used in geotechnical applications. Even though an environmental impact analysis was necessary, it was left out of the scope of the current project.

2. MATERIALS

An unpaved road material (URM) and two conventional base materials were used in this study. The URM was collected from a highway construction site in Caroline County, Maryland. Any debris and foreign materials in the soil were removed by hand and, by sieving through the 19 mm sieve. The soil is classified as poorly graded sand with gravel (SP) according to Unified Soil Classification System (USCS), and A-1-b (0) according to the American Association of State Highway and Transportation Officials (AASHTO) Classification System. The material did not exhibit any plasticity per ASTM D 4318.

Two base materials, Bank Run Gravel (BRG) and Graded Aggregate Base (GAB), used in highway construction in Maryland were tested as control soils. GAB meets the Maryland State Highway Administration (MDSHA) and AASHTO M-147 specifications and is termed as a high quality base material in Maryland. BRG is less commonly used in highway construction but was selected due its comparable particle size distribution with URM. GAB was excavated from an underground limestone mine located in Frederick, Maryland. The material was crushed upon mining, passed through a series of sieves to meet the gradations given in AASHTO M-147, and stockpiled in pits. BRG is originally mined from a sandstone mine located in Middletown, Maryland and was stockpiled in pits. Both materials were collected directly from the pits and delivered to the laboratory. The soils did not contain any organic matter or exhibit plasticity in Atterberg limit tests (ASTM D 4318). The fines content of BRG was 12%, and it was classified as SP-SM and A-1-b (0) according to the USCS and AASHTO, respectively. GAB included 4% fines by weight and was classified as SP and A-1-a (0) according to

the USCS and AASHTO, respectively. The two base materials and URM were stored in airtight buckets upon transfer to the laboratory in order to preserve their natural water content. Particle size distribution curves for the unpaved road material and conventional base materials are shown in Figure 1 along with the AASHTO M-147 and Virginia Department of Transportation (VDOT) specifications used for base construction. MDSHA specifications are the same of AASHTO M-147 specifications, thus not included in the figure. The obtained particle size distributions indicated that GAB satisfied the AASHTO M-147 and VDOT particle size distribution limits for highway bases whereas BRG and URM are tend to be outside of the limits. Physical properties of the two soils are summarized in Table 1.

The fly ashes used in this study were obtained from three power plants in Maryland: Brandon Shores, Paul Smith and Dickerson Precipitator. All three fly ashes consisted primarily of silt-size particles and contained 79 to 91% fines (passing the 75-mm sieve). Specific gravity (G_s) of fly ashes ranged between 2.17 and 2.37 per ASTM D 854. The fly ashes investigated in this study were classified as off-specification fly ashes (neither C or F type according to ASTM C 618) due their high loss on ignition (LOI>6). The chemical compositions of all three fly ashes are provided in Table 1. Since the three fly ashes do not have high cementing potential (i.e., low CaO), lime kiln dust (LKD) was used to initiate pozzolanic reactions for stabilization of the soil. LKD was obtained from Carmeuse Lime and Stone Company, Pittsburgh, Pennsylvania, and contained approximately 60% CaO by weight. The specific gravity of LKD is 2.97.

3. METHODS

3.1 California Bearing Ratio Test

The California bearing ratio (CBR) test is a penetration test for evaluation of the mechanical strength of road subrgrades and base courses. Soil-fly ash mixtures used in the CBR tests were prepared by mixing air-dried soil with a specified percent fly ash by weight. Fly ash percentages were selected as 10 and 20% to cover the typical range used in soil stabilization (ACAA 1999, Edil et al. 2002, Bin-Shafique et al. 2004). Initially, high percentages by weight of LKD (10 to 15%) were used as the activator for large volume use of this recycled material. However, due to extremely high strength values (CBR>150), more modest percentages of 2.5 and 5% by weight were selected. All specimens for the CBR tests were compacted at their optimum moisture contents (OMC) using the standard Proctor effort (ASTM D 698 Method B). Table 2 provides the OMC and maximum dry unit weights (γ_{dm}) of the mixtures based on compaction tests. After compaction, the specimens were extruded with a hydraulic jack, sealed in plastic wrap, and cured for 1, 7, and 28 days at 100% relative humidity and controlled temperature ($21 \pm 2\ ^{O}C$) before testing. CBR tests on specimens without fly ash/LKD were tested immediately after compaction (i.e., no curing). All CBR tests were conducted by following the methods outlined in AASHTO T-193 and ASTM D 1883. The specimens were unsoaked and the tests were performed with 1.27 mm/min strain rate using the Geotest Instrument S5840 Multi-Loader loading frame. The equipment had a maximum

loading capacity of 44.8 kN. Duplicate specimens were tested for CBR tests as quality control, and the averages of these two tests were reported as results.

3.2 Resilient Modulus Test

Resilient modulus test provides the stiffness of a soil under a confining stress and a repeated axial load. The procedures outlined in AASHTO T 307-99, a protocol for testing of base and highway base and subbase materials, were followed for resilient modulus tests. Unpaved road material and the two conventional base materials were mixed with fly ash and LKD at 10-20% and 2.5-5% by weight, respectively, and specimens of 101.6 mm in diameter and 230.2 mm in height were compacted in split molds at their OMC in eight layers using the standard Proctor energy. After compaction, the specimens were removed from the molds, sealed in plastic wrap, and were cured for 1, 7, and 28 days at 100% relative humidity and controlled temperature ($21 \pm 2\ ^{O}C$) before testing. The testing procedures were the same for BRG and GAB, except the specimens were compacted in split molds 152 mm in diameter and 305 mm in height.

A Geocomp LoadTrac-II loading frame and associated hydraulic power unit system was used to load the specimens. Conditioning stress was 103 kPa. Confining stress was kept between 20.7 and 138 kPa during loading stages, and the deviator stress was increased from 20.7 kPa to 276 kPa and applied 100 repetitions at each step. The loading sequence, confining pressure, and data acquisition were controlled by a personal computer equipped with RM 5.0 software. Deformation data were measured with

external linear variable displacement transducers (LVDTs) that had a measurement range of 0 to 50.8 mm.

Resilient moduli from the last five cycles of each test sequence were averaged to obtain resilient modulus for each load sequence. The resilient modulus of soil is usually nonlinear and is dependent on the stress level. This nonlinear behavior was defined in this study using the common model developed by Moosazadh and Witczak (1981):

$$M_R = K_1 \theta^{K_2} \quad (1)$$

where M_R is resilient modulus, K_1 and K_2 are constants, θ ($= \sigma_d + 3\sigma_c$) is bulk stress, σ_c is the isotropic confining pressure, and σ_d is the deviator stress. A summary resilient modulus (SM_R) was computed at a bulk stress of 208 kPa, following the guidelines provided in NCHRP 1-28A. The approach is also consistent with the suggestions in the recent mechanistic-empirical design guide on new and rehabilitated pavement structures to provide a constant resilient modulus for chemically stabilized materials (ARA 2004). The same bulk stress level was used in this study to verify the model. The power-model based values are summarized in Table 3. With few exceptions high R^2 values (R^2 >0.8) were obtained from regression analyses performed on the model, indicating that the mixtures have a response similar to that of granular materials.

To observe the effect of winter conditions on resilient moduli, some of the mixtures were subjected to strength and hydraulic conductivity tests after a series of freeze-thaw cycles. Specimens with varying fly ash and LKD contents and fly ash types

were compacted at their optimum moisture contents and 100% of maximum standard Proctor dry unit weight and following the procedures outlined in ASTM D 698. After 7 days of curing, the specimens were frozen in a temperature chamber at $-23 \pm 1\ ^{O}C$ for 24 hours and then thawed in a humidity chamber at 100% relative humidity and controlled temperature ($21 \pm 2\ ^{O}C$) for 23 hours per ASTM D 560. Specimens were frozen and thawed at zero overburden stress. The water content and resilient modulus were measured at the end of 4, 8, and 12 freeze-thaw cycles. Resilient modulus tests were conducted as described previously. Duplicate specimens were tested for most of the resilient modulus tests as quality control, and the averages of these two tests are reported as results.

3.3 Microscopy Analysis

Scanning electron microscopy (SEM) analyses were conducted on 7-day cured specimens. The specimens were initially treated with acetone, and a critical point drying apparatus was utilized to replace the acetone with CO_2. The specimens were held on an aluminum sample holder with adhesive tape. Later, they were coated with gold to minimize any charge build-up. Microstructure and chemical composition of the samples were examined under LEO 440 Model SEM using the energy dispersive X-ray (EDX) technique.

4. RESULT AND ANALYSIS

4.1 RESULTS OF CBR TESTS

The CBR test results are provided in Table 4 and Figure 2. Both BRG and GAB have higher CBR than unpaved road material (URM). The URM has significantly lower CBR than 50, a generally accepted limit for base applications (Asphalt Institute 2003), and thus required stabilization for use in highway construction. In all cases, CBR of stabilized mixtures is higher than that of URM and is comparable with or higher than the CBR of the two conventional base materials even after 1 day of curing. The data also indicate that mixing with only fly ash is not sufficient enough to increase the strength due to its non-cementitious nature (i.e., low free lime, CaO) of the ashes, and addition of a lime source, such as LKD, is necessary to start pozzolanic reactions. The SEM photographs in Figure 3 show the coating of fly ash particles as a result of cement or lime kiln dust (LKD) addition, which may be an indicator of an increase in CBR (Conner 1990). Relatively higher amounts of calcium are evident as a result of the addition of LKD, as shown in the EDX plots of Figure 4.

CBR of LKD amended soil-fly ash mixtures also increase with increasing curing time (Figure 2). As LKD is mixed with moist soil, the hydration of calcium oxide (CaO) causes the formation of ($Ca(OH)_2$), and disassociation of ($Ca(OH)_2$) favors dissolution of silica and alumina in fly ash. This phenomenon gives rise to formation of calcium silicate hydrate (CSH) and calcium aluminate silicate hydrate gels (CASHs) around soil particles. It is speculated that the delayed release of CaO in LKD caused these increases and the temperature of the curing chamber and availability of 100% relative humidity

also contributed to the cementitious reactions. The increase in CBR after 1 day of curing is relatively modest; however, CBR of the 7 and 28-day cured specimens increased up to 6 and 7 times, respectively. Similar increases in strength with increasing curing period were reported by previous researchers (Vishwanathan et al. 1997, Arora and Aydilek 2005, Guney et al. 2006).

Two different amounts of lime kiln dust (LKD) were added to the soil specimens. As seen in Figure 5, an increase in LKD amount increases the CBR values significantly due to cementation of the particles by the LKD. The rate of increase is higher initially, and increasing the LKD amount from 0% to 2.5% by weight had a greater effect than increasing the amount from 2.5% to 5% by weight. The CBR of unpaved road material increases at least three and five times due to addition of 2.5% and 5% LKD by weight, respectively. Similar trends were observed by Consoli et al. (2001) during strength testing of soils stabilized with fly ash and carbide lime. The CBR of all 7-day and 28-day cured specimens tested in the current study exceeds 50.

In order to evaluate the effect of mixture chemical composition on observed strength, a paired t-test was conducted at significance level of 0.05, corresponding to $t_{critical} = t_{cr} = 2.06$ for CBR test results and $t_{cr}=2.09$ for resilient modulus test results. CBR values are plotted against CaO content, and CaO/SiO_2 and $CaO/ (SiO_2 + Al_2O_3)$ ratios and fineness of fly ash in Figure 6. The two ratios stay below 1.0, and are well below 3 and 2.5, the ratios documented for Portland cement (Table 4). As expected, the data in Figure 6 suggest that CBR increases with increasing CaO content and CaO/SiO_2 and $CaO/(SiO_2 + Al_2O_3)$ ratios and the best fit curves to the data produced modest R^2 values (0.79, 0.66 and 0.73, respectively). Janz and Johansson (2002) indicated that the

CaO/SiO_2 ratio can be a good indicator of pozzolanic reactions, and larger CaO/SiO_2 generally yields higher strength values. Tastan et al. (2009) showed that the cementing potential of materials can be strongly related to CaO content of the binder as well to these ratios. Tastan et al. (2009) also reported that the CaO/SiO_2 and $CaO/ (SiO_2 + Al_2O_3)$ ratios typically range from 0.5 to 1.0 and from 0.4 to 0.7, respectively, for fly ash-stabilized subgrade soils. These observations are, in general, consistent with the findings obtained in the current study. Fineness of fly ash refers to particles retaining on the 45 μm sieve (U.S. No. 325 standard sieve size) and defines the surface area of fly ash particles present in per unit weight. If the fly ash is self-cementitious (i.e., Class C), higher fineness percentages typically enhance the reaction rate which result in faster gain of strength at earlier stages. As seen in Figure 6d, the correlation between the fineness and CBR is poor ($t < 1.96$), mainly due to non-cementitious nature of the Maryland fly ashes.

Attempts were also made to relate CBR to three commonly used ratios in cement production: silica ratio (SR), alumina ratio (AR) and lime saturation factor (LSF). The silica ratio ($SR=SiO_2/ (Al_2O_3 + Fe_2O_3)$) represents the required energy to combine raw materials in a stabilization application. When SR increases, it becomes harder to combine the raw materials whereas a decrease in SR suggests an increase in the ability of solid materials to become liquid. The alumina ratio (Al_2O_3/Fe_2O_3) is important as it alumina-to-iron ratio in cement is known to be an indicator of sulfate resistance, heat generation, and admixture compatibility issues. The lime saturation factor (LSF) is dependent on the C_3S-to-C_2S ratio in the finished cement, where the early and delayed age strength development is governed by C_3S and C_2S, respectively (PCA 2009). LSF typically

remains between 0.95 and 0.98 for Portland cement and higher LSF indicates the presence of excess free lime which is likely to remain unreacted in the mixture (Taylor 1997). No clear trends or correlations can be visualized in Figure 7. This is not surprising as these ratios are generally not used as indicators of pozzolanic reactions. As mentioned before, increase in fly ash content only does not change stresses and no correlation can be observed between fly ash percentage and CBR (Figure 7d).

4.2 RESULTS OF RESILIENT MODULUS TESTS

4.2.1 Effects of Curing Time, LKD Addition on Summary Resilient Moduli and Plastic Strain

Summary resilient moduli of the tested specimens are given in Table 4. GAB has the highest CBR of all three unstabilized materials due to its high gravel content. The measured SM_R of GAB falls into the range of suggested SM_R for SP or SP-SM soils reported in the Mechanistic-Empirical Design Guide (165 to 228 MPa), whereas the same is not true for BRG and URM (ARA 2004). Similar to CBR data, URM has low summary resilient modulus, justifying the need for stabilization with a calcium-rich binder. The order of SM_R is compatible with that of CBR; however, a strong correlation was not obtained when CBR was plotted against SM_R (Figure C1 in Appendix). Camargo (2008) also attributed the difference to the application of different magnitudes of deformations to the specimens during testing and measurement of two separate

geomechanical properties (i.e., small deformations and measurement of stiffness during resilient modulus test versus large deformations and bearing capacity determination during CBR test).

Attempts were also made in the past to correlate CBR to resilient modulus data by using two well-known empirical equations by Powell et al. (1984) and Haukelom and Foster (1960), respectively:

$$SM_R = 7.6\text{CBR}^{0.64} \quad (2)$$

$$SM_R = 10\text{CBR} \quad (3)$$

where SM_R is summary resilient modulus in MPa. As seen in Figure 8, both equations overpredict the measured resilient modulus data. Similar observations were also made by Sawangsuriya and Edil (2005) and Acosta et al. (2006). Due to low correlations observed between CBR and SM_r (R^2=0.33 and 0.32 for 1 and 7-day cured specimens, respectively), no further attempt was made to develop an empirical equation to predict resilient modulus from the CBR data.

Average plastic strains were calculated for all base materials during resilient modulus testing using data from the LVDTs. Plastic strain for a resilient modulus test was calculated as the sum of the plastic strains for each loading sequence, excluding the plastic strains in the conditioning phase. The plastic strains ($\varepsilon_{plastic}$) for two Maryland base materials and URM, along with stabilized soils are summarized in Table 3. BRG and GAB showed average plastic strains of 1% and 0.94%, respectively, whereas URM

showed an average plastic strain of 0.97%. The calculated strains for the high quality Maryland base materials are comparable with those of conventional base aggregates reported in the literature (Camargo 2008). The high plastic strain of BRG and URM is attributed to their relatively higher sand content (68% and 67%, respectively) as compared to GAB (51%), consistent with the observations of Camargo (2008).

A variation of SM_R with curing time is shown in Figure 9. SM_R increases with increasing curing time. The average change in SM_R caused during the 1-day curing was about 35%, and increasing the curing time from 0 to 1 day had a slightly greater effect than increasing the curing time from 1 to 7 or 7 to 28 days (assuming that the SM_R of mixtures were no different than that of URM at 0 days). Curing of specimens longer periods also resulted in lower plastic strains (Table 3). Similar to CBR test results, the SM_R increased with increasing LKD amount due to cementitious reactions formed between fly ash and LKD, and the summary resilient modulus of unpaved road material increased 1.4 to 4 times as a result of stabilization (Figure 5). The SM_R ranged between 157 and 510 MPa, and the maximum SM_R was recorded for BS20+5 LKD (unpaved road material mixed with 20% Brandon Shores fly ash and 5% LKD by weight) upon 28 days of curing. It can be concluded that an LKD content of 5% by weight leads to reasonably high SM_R values and addition of LKD beyond that amount may not be necessary. Moreover, Cross and Young (1997) reported higher initial cracking of recycled pavement materials with increasing cementitious fly ash contents. On the other hand, the maximum LKD content was set at 5% in the current study solely considering the cost-effectiveness; however, additional testing is required to obtain the LKD contents beyond which SM_R no longer increases.

Table 3 summarizes the two constants, K_1 and K_2, for the resilient modulus power function model along with the best fit correlation coefficients. The resilient modulus is plotted versus bulk stresses for the mixtures prepared with two of the fly ashes in Figure 10. An increase in resilient modulus with increasing bulk stress is observed for all specimens, which is in agreement with the behavior generally observed for granular soils (AASHTO T-307-99). The optimum moisture content of the mixtures compacted using standard Proctor effort range from 9% to 13%, and the difference between the maximum dry densities of the specimens is insignificant (Table 2). Therefore, the difference in resilient modulus is attributed solely to the variation in LKD content. As expected, resilient modulus increases with increasing LKD content at a given bulk stress due to production of more cementitious compounds with LKD addition. Figure 10 further suggests that fly ash generally acts as a bulking agent and does not contribute to resilient modulus, as the resilient modulus at a given LKD content and bulk stress either stays the same or decreases with increasing fly ash content, with the exception of the specimen prepared with 10% Paul Smith fly ash. LKD addition caused an increase in SM_R but also decreased the plastic strain of URM. In general, addition of non-cementitious fly ash did not cause significant changes in plastic strains (Table 3).

Figure 11 suggests that SM_R tends to increase with increasing mixture CaO content, and CaO/SiO_2 and $CaO/(SiO_2 + Al_2O_3)$ ratios, even though CaO/SiO_2 ratio is the only one that exhibited correlation with resilient modulus ($t > t_{critical} = 2.09$). Furthermore, SM_R was not correlated with silica ratio, alumina ratio, lime saturation factor, or fly ash percentage (Figure 12).

4.2.2 Effect of Freeze-Thaw on Summary Resilient Moduli

Stabilized highway construction material should be able to resist against climatic stresses, especially freeze-thaw cycles (TFHRC 2002). Subjecting the specimens to strength after freeze-thaw (F-T) cycles and recording the change in weight have been reported as indicators of durability. However, the evaluation of durability by weight loss as a result of freeze-thaw cycles (ASTM D 560) has been dropped by some state agencies as the procedure is overly severe, and does not totally simulate field conditions. Previous research indicates that 8 to 12 cycles of freezing and thawing could be considered adequate in investigating the effect of F-T cycles on different engineering parameters including strength (Zaman and Naji 2003).

In this study, six different mixtures were cured for 7 days as normally practiced in pavement construction. The specimens were subjected to resilient modulus tests following a series of freezing and thawing cycles. The test results are summarized in Table 6 and Figure 13. The summary resilient modulus ratio (SM_R Ratio = SM_{Rn}/ SM_{Ri}) is the ratio of summary resilient modulus after n freeze-thaw cycles (SM_{Rn}) to the initial summary resilient modulus (SM_{Ri}).

The specimens either gain strength or lose only 3 to 12% of their initial resilient modulus after four cycles, and then SM_R starts to decrease indicating the detrimental effects of freeze and thaw cycles. The highest decreasing rate of SM_R can be observed between the fourth and eighth cycle, and the specimens lose 31 to 67% of their initial moduli after twelve cycles of freezing and thawing. Similar trends were observed for

unbound materials by Simonsen et al. (2002). Rosa (2006) also reported a 20 to 66% reduction in SM_R of various coarse and fine-grained soils.

The effect of freeze-thaw on resilient modulus can be explained in terms of retardation or acceleration of the cementitious reactions. Freezing action retards the cementitious reactions, which causes a reduction in stiffness: conversely, thawing action contributes to an increase in SM_R via accelerating the cementitious reactions. The freezing and thawing compensated each other in first four cycles of soil specimens. It is believed that between cycles of 4 and 12, freezing caused the breaking of the cement bonds in the mixture and resulted in a significant decrease in SM_R. As compared to previous studies conducted on sandy soils and soils with some plasticity (Arora and Aydilek 2005, Rosa 2006, Camargo 2008), a larger change can be observed in the moduli of specimens tested in the current study. This may be attributed to the high gravel content and nonplastic nature of the current mixtures, which have relatively high porosity and susceptibility to frost action.

The effect of freeze-thaw is consistent with the volume changes of specimens. The volume changes remain nearly constant within the first four cycles, after which increases significantly evidenced by the changes in water contents shown in Figure 14. It is believed that freezing process caused breakage of the chemical bonds and allowed water to freely penetrate into the pores, thereby causing large increases in water contents, i.e., up to 89% increase in water content after 12 cycles of freezing and thawing.

5. PRACTICAL IMPLICATIONS

5.1 Highway Base Design

CBR and resilient modulus test results were used to estimate the thickness of the base layer in a pavement by following the procedures defined in the AASHTO Guide (1993). Low traffic (Case I) and high traffic (Case II) conditions were simulated by using 5 million and 50 million equivalent single-axle loads (ESALs or W_{18}), respectively. The overall standard deviation (S_o) and reliability (Z_R) were assumed to be 0.35 and 95%, respectively. Structural numbers (SN) for two traffic conditions were back-calculated using Equation 2.

$$\log(W_{18}) = Z_R \cdot S_0 + 9.36 \cdot \log_{10}(SN+1) - 0.20 + \frac{\log_{10}(\Delta PSI)/(4.2-1.5)}{0.4 + 1094/(SN+1)^{5.19}} + 2.32 \cdot \log_{10}(M_R) - 8.07$$

(4)

where ΔPSI is design serviceability loss and M_R is the roadbed material effective resilient modulus. The values were selected as 1.9 and 34.5 MPa, respectively, based on Huang (1993). An asphalt layer thickness of 102 mm for Case I and 152 mm for Case II was selected. The resilient modulus of asphalt was assumed to be 2965 MPa, which corresponded to a structural coefficient of a_1 = 0.44 according to the AASHTO Guide (1993). A resilient modulus of 103 MPa (corresponding to a structural coefficient of a_3 =

0.11) and a thickness of 406 mm (D_3) were assumed for the subbase layer for both cases. The structural coefficient of the base layer (a_2) was calculated for its corresponding CBR or SM_R values using the procedure given in the AASHTO Guide (1993). The CBR and SM_R of 28-day cured specimens were used due to their common use in highway construction. Finally, the base thicknesses were calculated using the following formula:

$$D_2 = \frac{SN - a_1 D_1 - a_3 D_3 m_3}{a_2 m2} \quad (5)$$

where m_2 and m_3 are the drainage modification factors for the base and subbase layer, respectively, and were chosen as 1.2, 1.0, 0.8, 0.6 for excellent, good, fair, poor drainage conditions, respectively, within the pavement system (Huang 1993). Table 7 shows the required base thicknesses for Cases I and II under excellent drainage conditions. Furthermore, the required base thickness decreased with increasing resilient modulus, as seen in Figure 15. The change in drainage conditions require higher base thickneeses as reflected in Tables E.1-E.3 in Appendix E.

The base layer thicknesses of all stabilized mixtures based on SM_R are consistently lower than that of unpaved road material and generally comparable or lower than that of the two typical Maryland base materials. Increase in fly ash content at fixed LKD content results in higher base thicknesses due to non-cementitious nature of the ashes used. In addition, a decrease in amount of lime kiln dust (LKD) and increase in traffic load required thicker base layers in highway construction. An analysis of curing time effect on required base thicknesses were not conducted; however, it is well-known

that increase in curing time is likely to yield lower base thickness since the specimens gain strength at later stages. As discussed before, winter conditions generally lead to a decrease in strength of lime-treated mixes. This would generally require larger base thicknesses, in particular after 4 cycles of freezing and thawing as presented in Tables D1 and D2 and Figure D1 of Appendix. However, it should be noted that the climatic stresses may have unexpected effects on the soil mixtures, particularly in short term (i.e., during construction), and therefore precautions should be taken to protect specimens from in-situ freezing conditions.

5.2 Cost Calculations

A simple cost analysis, considering the material, hauling and transportation costs only, was performed to on all soils and mixtures. In the current study, three different fly ashes and one type of lime kiln dust were used at varying percentages by weight. The road construction site was assumed to be the Route 1 expansion project site located in College Park, Maryland. The fly ashes were available at no cost. The Brandon Shores, Paul Smith and Dickerson power plants were located about 43 km, 101 km, 52 km, respectively, from the construction site. The URM, a material commonly used in unpaved road construction in Caroline County, Maryland, was available at $4/t. The distance between the construction site and URM plant was 64 km. Lime kiln dust material was available from the manufacturer for about $16/t. However the closest lime kiln dust supplier was in Pittsburgh, PA which was 390 km away from the construction site. The GAB plant was 77 km away from the construction site, and the cost of the GAB material was $10/t. The

BRG plant was 83.2 km away from the construction site and the cost of the BRG materials was $10/t. A fuel charge of $0.5/t and hauling costs of $0.25/t were assumed for all materials.

Lane widths in the United States can range from 3 m (low volume roads) to 5 m (highway ramps) in width, and a typical design width of 4 m was selected for the Route 1 expansion project. To represent a typical roadway, a four-lane roadway was considered with two 2-m shoulders. The detailed cost analysis summarized in Table 8 indicates that using stabilized URM in a roadway base application has a clear advantage over using other conventional earthen base materials.

The factors that mainly affect the cost are traffic volume and drainage conditions. The required base layer thicknesses increase due to a decrease in drainage quality of highways (Table E4-E6). Moreover, increasing traffic volume increases the total construction cost increases significantly (Figure E1). Addition of the activator (i.e., LKD) decreases the cost, even under low drainage conditions, due to its positive effect on required base thickneesses.

6. CONCLUSIONS

Roadways are one of the largest construction fields, and reuse of suitable waste materials in their construction can provide significant cost savings while meeting the objectives of the United States Federal Highway Administration Green Highways Partnerships initiative. A laboratory study was conducted to investigate the feasibility of reusing chemically stabilized road surface material in construction of highway bases. Non-cementitious off-spec high carbon fly ash was activated lime kiln dust and used to stabilize an unpaved road material (URM) collected from Maryland. The effects of lime kiln dust (LKD) and fly ash addition, and curing time on strength and stiffness of highway bases were studied. The effects of winter conditions on stiffness were examined by performing resilient modulus tests on the specimens after a series of freeze-thaw cycles. The base thicknesses were calculated for all mixture designs by using their CBR and summary resilient moduli (SM_R) values. The observations are summarized as follows:

1) Addition of lime kiln dust (LKD) and curing of specimens increase CBR and SM_R significantly, whereas increase in fly ash content generally decreases the strength and stiffness due to the non-cementitious nature of the high carbon Maryland fly ash and that the fact that ash acts as a bulking agent. Almost all specimens have CBR values higher than 50, a limit typically considered for construction of base layers. Measured SM_Rs were comparable with the ones reported for highway bases in previous studies.

2) Both BRG and GAB exhibited higher CBR and SM_R than unpaved road material (URM). The order of SM_R was also compatible with that of CBR in spite of the differences in nature of the two test methods. The two Maryland base materials, BRG and GAB, had comparable plastic strains with those documented for conventional base aggregates in the literature. In general, lower plastic strains were obtained by addition of LKD as well as with increasing curing time whereas fly ash addition did not affect the strains significantly.
3) CBR increased with increasing CaO content as well as with CaO/SiO_2 and $CaO/(SiO_2 + Al_2O_3)$ ratios; however, these parameters could not be correlated with the SM_R. Moreover, silica and alumina ratios and lime saturation factor, three common parameters for definition of cementitious activity, are not likely to affect the CBR or SM_R.
4) Early stages of freezing and thawing did not cause detrimental effects on resilient modulus; however, the unpaved road materials stabilized with LKD and fly ash lost 31 to 67% of their initial moduli after twelve cycles of freezing and thawing. Such high changes in SM_R are attributed to the frost susceptibility of mixtures due to their high gravel content and nonplastic nature
5) Lower base thickness would be required if higher amount of lime kiln dust materials is used during construction of the base layer. It should also be noted that an increase in LKD content and decrease in traffic load are likely to decrease the required thicknesses.

6) Significant cost reduction be expected by stabilizing unsuitable roadway materials with high carbon fly ash and lime kiln dust while the total cost is mainly affected by the traffic volume and pavement drainage conditions

REFERENCES

AASHTO Guide (1993). "*Guide for Design of Pavement Structures*", American Association of State Highway and Transportation Officials, Washington, D.C.

ACAA (2003). "*2001 Coal Combustion Product Production and Use*", American Coal Ash Association, Denver, Colorado

ARA (2004). "Guide for Mechanistic-Empirical Design on New and Rehabilitated Pavement Structures," NCHRP Project 1-37A. Prepared for National Cooperative Highway Research Program, Washington, D.C.

Arora, S. and Aydilek, A.H. (2005). "Class F Fly Ash Amended Soils as Highway Base Materials", *Journal of Materials in Civil Engineering,* Vol. 17, No. 6, pp. 640-649.

Asphalt Institute (2003). "*Thickness Design –Highways and Streets*", Manual Series, No. 1, Asphalt Institute, Lexington, Kentucky, 110 p.

Bin-Shafique, S., Edil, T., Benson, C., and Senol, A. (2004). "Incorporating a fly ash stabilized layer into pavement design-Case study." *Geotechnical engineering*, Institution of Civil Engineers, London, Vol. 157, No. GE4, 239–249.

Buhler, S.R. and Cerato, A.B. (2007). "Stabilization of Oklahoma Expansive Soils Using Lime and Class C Fly Ash", *ASCE Geotechnical Special Publication,* 162, pp. 1-10.

Camargo, F.F. (2008). "Strength and Stiffness of Recycled Base Materials Blended with Fly Ash", M.S. Thesis, University of Wisconsin-Madison, 123 p.

Conner, J.R. (1990). "*Chemical Fixation and Solidification of Hazardous Wastes*", Van Nostrand Reinfold, New York, 692 p.

Consoli, N. C., Prietto P. D. M., Carraro, J. A. H., and Heineck, K., S. (2001). "Behavior of Compacted Soil-Fly Ash-Carbide Lime Mixtures." *Journal of Geotechnical and Geoenvironmental Engineering*, Vol. 127, No. 9, pp. 774-782.

Cross, S. A. and Young, D. A. (1997). Evaluation of Type C Fly Ash in Cold-in-Place Recycling, *Journal of the Transportation Research Board,* 1583, pp. 82–90.

DiGioia, A. M. and Nuzzo, W. L. (1972). "Fly Ash as Structural Fill," *J. Power Div.,* ASCE, New York, Vol. 98 (1), pp. 77-92.

Edil, T.B., Acosta , A.A., and Benson, C.H. (2006). "Stabilizing Soft Fine-Grained Soils with Fly Ash", *Journal of Materials in Civil Engineering*, Vol. 18, No. 2, pp. 283-294.

Edil, T. B., Benson, C., Bin-Shafique, M., Tanyu, B., Kim, W. and Senol, A. (2002). "Field evaluation of construction alternatives for roadways over soft subgrade", *Journal of the Transportation Research Board,* 1786, pp. 36-48.

Gray, D. H., and Lin, Y. K. (1972). "Engineering Properties of Compacted Fly Ash,"*J. of Soil Mech. and Found. Engrg.*, ASCE, New York, Vol. 98 (4), pp. 361-380.

Guney, Y., Aydilek, A.H., and Demirkan, M.M. (2006). "Geoenvironmental Behavior of Foundry Sand Amended Mixtures for Highway Subbases", *Waste Management,* Vol. 26, pp. 932-945.

Hatipoglu, B., Edil, T., and Benson, C. (2008). "Evaluation of base prepared from road surface gravel stabilized with fly ash", *ASCE Geotechnical Special Publication,* 177, pp. 288-295.

Heukelom, W., and Foster, C. (1960). “Dynamic Testing of Pavements.” *Journal of Soil Mechanics and Foundation Division, Vol.* 86, No. 1, pp.1–28.

Huang, Y. H. (1993). “*Pavement Analysis and Design*”, Prentice-Hall, Inc., New Jersey, 805 p.

Janz, M. and Johansson, S.-E. (2002). "The Function of Different Binding Agents in Deep Stabilization," Report 9. Swedish Deep Stabilization Research Centre, Linkoping, Sweden.

Kumar, A., Walia, B.S., and Bajaj, A.(2007). “Influence of Fly Ash, Lime, and Polyster Fibers on Compaction and Strength Properties of Expansive Soils”, *Journal of Materials in Civil Engineering,* Vol. 19, No. 3, pp. 242-248.

Li, L., Benson, C. H., Edil, T. B., Hatipoglu, B., and Tastan, E. (2007). “Evaluation of recycled asphalt pavement material stabilized with fly ash”, *ASCE Geotechnical Special Publication (CD-ROM)*, 169.

Moosazedh, J., and Witczak, M. (1981). “Prediction of Subgrade Moduli for Soil that Exhibits Nonlinear Behavior”, *Journal of the Transportation Research Board,* 810, pp. 10-17.

PCA (2009). Portland Cement Association, www.cement.org

Powell, W., Potter, J., Mayhew, H., and Nunn, M. (1984). *The Structural* D*esign of Bituminous Roads*, *TRRL Laboratory Report 1132*, Transportation and Road Research Laboratory, Crowthorne, Berkshire, U.K, 62 p.

Rosa, M. (2006). “Effect of Freeze and Thaw Cycling on Soils Stabilized using Fly Ash,” *MS Thesis*, University of Wisconsin-Madison, Madison, WI.

Saylak, D., Mishra, S.K., Mejeoumov, G.G., and Shon, C.C. (2008). "Fly Ash-Calcium Chloride Stabilization in Road Construction", *Proceedings of 87th Annual Meeting (CD ROM)*, Transportation Research Board, Washington, D.C.

Sawangsuriya, A. and Edil, T. B. (2005), "Evaluating stiffness and strength of pavement materials, geotechnical engineering." *Geotechnical Engineering*, Institution of Civil Engineers, London, Vol. 158, No. GE4, 217–230.

Shao, L., Liu, S., Du, Y., Jing, F. and Fang, L. (2008). "Experimental Study on the Stabilization of Organic Clay with Fly Ash and Cement Mixed Method", *ASCE Geotechnical Special Publication,* 179, pp.20-27.

Simonsen, E., Janoo, V., and Isacsson, U. (2002). "Resilient properties of unbound road material during seasonal frost conditions", *Journal of Cold Region Eng.*, 16(1), pp. 28-50.

Tastan, O., Benson, C.H., Edil, T.B., and Aydilek, A.H. (2009). "Stabilization of Organic Soils with Fly Ashes", *Journal of Geotechnical and Geoenvironmental Engineering*, submitted.

Taylor, H.F.W. (1997). "Cement Chemistry", Second edition, Thomas Telford, Inc.

Vishwanathan, R., Saylak, D., and Estakhri, C. (1997). "Stabilization of Subgrade Soils Using Fly Ash", *Proceedings of the Ash Utilization Symposium, CAER*, Kentucky, pp. 204-211.

Wen, H., Baugh, J., and Edil, T. (2007). "Use of Cementitious High Harbon Fly ash to Stabilize Recycled Pavement Materials as Pavement Base Material", *Proceedings of 86th Annual Meeting (CD ROM)*, Transportation Research Board, Washington, D.C.

Wen, H., Warner, J., and Edil, T. (2008). "Laboratory comparison of crushed aggregate and recycled pavement material with and without high-carbon fly ash", *Proceedings of 87th Annual Meeting (DVD)*, Transportation Research Board, Washington, D.C.

Zaman, M., and Naji, K. (2003). "Effect of freeze-thaw cycles on class C fly ash stabilized aggregate base", *Proceedings of 82nd Annual Meeting (CD ROM)*, Transportation Research Board, Washington, D.C.

TABLES

TABLE 1a. Index properties of the materials used in current study

Sample	C_u	Gs	w_{opt} (%)	γ_d (kN/m^3)	LL (%)	PI (%)	Gravel Content (%)	Fines Content (<75 μm) (%)	Fineness (>45 μm) (%)	Classification	
										USCS	AASHTO
BRG	25	2.52	8.0	20.4	NP	NP	20	12	0	SP-SM	A - 1 – b (0)
GAB	39	2.81	4.1	23.8	NP	NP	45	4	0	SP	A - 1 – a (0)
URM	6.7	2.64	13.4	18.8	NP	NP	30	3	0	SP	A - 1 – b (0)
BS	0.43	2.17	–	–	NP	NP	–	91	25	ML	A - 2 – 4 (0)
PS	11	2.2	–	–	NP	NP	–	80	51	ML	A - 2 – 4 (0)
DP	3.6	2.37	–	–	NP	NP	–	79	34	ML	A - 2 – 4 (0)

.

TABLE 1b. Chemical composition of the fly ashes. Concentrations of major minerals were determined by X-ray fluorescence spectroscopy analysis. All concentrations are in percentage by weight.

Fly ash	Chemical Composition												
	LOI (%)	SiO_2 (%)	Al_2O_3 (%)	Fe_2O_3 (%)	CaO (%)	K_2O (%)	TiO_2 (%)	MgO (%)	Na_2O (%)	Cr_2O_3 (%)	P_2O_5 (%)	SrO (%)	BaO (%)
BS	13.4	45.1	23.1	3.16	7.8	1.7	1.4	0.8	0.3	0.02	0.09	0.06	0.06
PS	10.7	50.8	26.9	5.5	0.7	2.2	1.5	0.6	0.2	0.02	0.2	0.03	0.05
DP	20.5	34.9	24.4	12.6	3.2	1.1	1.3	0.5	0.3	0.03	1.0	0.2	0.11

BRG: Bank run gravel, GAB: Graded aggregate base, URM: Unpaved road material, PS: Paul Smith fly ash, DP: Dickerson Precipitator fly ash, BS: Brandon Shores fly ash, LOI: Loss on ignition. Gs: Specific gravity, C_u: coefficient of uniformity, C_c: coefficient of curvature, w_{optm}: optimum water content, γ_{dmax}: maximum dry unit weight, LL: liquid Limit, PL: plastic limit, NP: Nonplastic.

TABLE 2. Legend and compositions of the mixtures.

Legend of Mixtures	Fly Ash Content (%)	LKD Content (%)	Optimum Water Content (%)	Maximum Dry Unit Weight (kN/m^3)
BRG	0	0	8.0	20.4
GAB	0	0	4.1	23.8
URM	0	0	13.4	18.8
10 BS + 2.5 LKD	10	2.5	10	19.2
10 BS + 5 LKD	10	5	9.5	19.2
20 BS + 2.5 LKD	20	2.5	10	18.5
20 BS + 5 LKD	20	5	13	17.4
10 PS + 2.5 LKD	10	2.5	9.0	18.8
10 PS + 5 LKD	10	5	10	18.8
20 PS + 2.5 LKD	20	2.5	12	17.3
20 PS + 5 LKD	20	5	13	17.0
10 DP + 2.5 LKD	10	2.5	9.0	19.1
10 DP + 5 LKD	10	5	10	19.4
20 DP +2.5 LKD	20	2.5	10	18.1
20 DP + 5 LKD	20	5	12	18.0

BS: Brandon Shores fly ash, PS: Paul Smith fly ash, DP: Dickerson Precipitator fly ash, LKD: Lime kiln dust, BRG: Bank run gravel, GAB: Graded aggregate base, URM: Unpaved road gravel. The numbers that follow the fly ashes and LKD indicate the percentages by weight of admixtures added to the soil.

TABLE 3. Power model fitting parameters and measured plastic strains for resilient modulus tests.

Fly Ash Type	Fly Ash Content (%)	LKD Content (%)	K_1	K_2	$\varepsilon_{plastic}$ (%)	K_1	K_2	$\varepsilon_{plastic}$ (%)	K_1	K_2	$\varepsilon_{plastic}$ (%)
			1-Day Cured or no curing for BRG, GAB and URM			7-Day Cured			28-Day Cured		
Brandon Shores	10	2.5	3260	0.57	0.83	6593	0.53	0.62	1412	0.93	0.49
	10	5	6470	0.49	0.67	3595	0.69	0.5	1636	0.81	0.49
	20	2.5	3260	0.57	0.74	1873	0.75	0.73	1300	0.84	0.63
	20	5	85000	0.46	0.67	4225	0.59	0.59	36473	0.2	0.47
Paul Smith	10	2.5	5896	0.49	0.63	8193	0.43	0.61	10670	0.33	0.54
	10	5	6341	0.43	0.73	12410	0.41	0.4	16508	0.38	0.34
	20	2.5	6022	0.47	1.07	4904	0.52	0.66	3623	0.57	0.66
	20	5	8158	0.42	0.83	12876	0.33	0.59	15629	0.32	0.49
Dickerson Precipitator	10	2.5	3220	0.61	0.76	3973	0.55	0.72	2047	0.87	0.44
	10	5	4768	0.56	0.59	4800	0.55	0.42	10310	0.53	0.29
	20	2.5	3169	0.62	0.7	8830	0.41	0.57	2689	0.72	0.54
	20	5	6500	0.49	0.56	11329	0.41	0.43	7367	0.54	0.4
BRG	0	0	2450	0.60	1.0	-	-	-	-	-	-
GAB	0	0	7700	0.40	0.94	-	-	-	-	-	-
URM	0	0	1623	0.71	0.97	-	-	-	-	-	-

LKD: Lime kiln dust

TABLE 4. CBR and summary resilient modulus values

Soil or Fly Ash Type	Fly Ash Content (%)	LKD Content (%)	CBR (%)			SM_R (MPa)		
			1 Day Cured	7 Days Cured	28 Days Cured	1 Day Cured	7 Days Cured	28 Days Cured
Brandon Shores	10	2.5	70	108	> 131	157	228	260
	10	5	73	142	> 156	179	245	274
	20	2.5	45	112	> 121	147	157	169
	20	5	76	133	> 152	215	284	510
Paul Smith	10	2.5	83	115	> 120	189	230	243
	10	5	95	135	> 164	216	350	418
	20	2.5	34	71	100	172	198	207
	20	5	60	87	>105	238	278	323
Dickerson Precipitator	10	2.5	44	69	> 120	174	180	277
	10	5	93	129	> 143	219	322	433
	20	2.5	65	84	111	183	217	243
	20	5	82	110	> 134	241	312	326
BRG	0	0	27			130		
GAB	0	0	42			206		
URM	0	0	24			127		

BRG: Bank run gravel, GAB: Graded aggregate base, URM: Unpaved road gravel, LKD: Lime kiln dust

TABLE 5. Chemical compositions of mixtures prepared with three different fly ashes

Chemical Constituents	BS (%)	PS (%)	DP (%)	Type I Portland Cement (%)	Lime kiln dust (%)	Mixtures Prepared with BS				Mixtures Prepared with PS				Mixtures Prepared with DP			
						10BS+ 2.5L	10BS+ 5L	20BS+ 2.5L	20BS+ 5L	10PS+ 2.5L	10PS+ 5L	20PS+ 2.5L	20PS+ 5L	10DP+ 2.5L	10DP+ 5L	20DP+ 2.5L	20DP+ 5L
SiO_2	45.1	50.8	34.9	22	7.5	37.6	32.6	40.9	37.6	42.1	36.4	46	42.1	29.4	25.8	31.9	29.4
Al_2O_3	23.1	26.9	24.4	5	2.7	19	16.3	20.8	19	22	18.8	24.2	22	20.1	17.2	22	20.1
Fe_2O_3	3.2	5.5	12.6	3	1.1	2.7	2.5	2.9	2.7	4.6	4	5	4.6	10.3	8.8	11.3	10.3
CaO	7.8	0.7	3.2	67	61.6	18.6	25.7	13.8	18.6	12.9	21	7.5	12.9	14.9	22.7	9.7	14.9
MgO	0.8	0.6	0.5	1	2.5	1.2	1.4	1	1.2	1	1.2	0.8	1	0.9	1.2	0.7	0.9
SiO_2+ Al_2O_3 + Fe_2O_3	71.4	83.2	71.9	30	11.3	59.3	51.3	64.7	59.3	68.8	59.2	75.2	68.8	59.8	51.7	65.2	59.8
Silica Ratio (SR)	1.7	1.6	0.9	2.8	2	1.7	1.7	1.7	1.7	1.6	1.6	1.6	1.6	1	1	1	1
LSF	0.05	0.006	0.03	1	2.6	0.1	0.2	0.1	0.1	0.1	0.2	0.05	0.1	0.1	0.2	0.1	0.1
Alumina Ratio (AR)	7.3	4.9	1.9	1.7	2.5	6.9	6.6	7.1	6.9	4.8	4.7	4.8	4.8	2	2	1.9	2
CaO/SiO_2	0.2	0.01	0.1	3	8.2	0.5	0.8	0.3	0.5	0.3	0.6	0.2	0.3	0.5	0.9	0.3	0.5
CaO/ (SiO_2+Al_2O_3)	0.1	0.01	0.05	2.5	6	0.3	0.5	0.2	0.3	0.2	0.4	0.1	0.2	0.3	0.5	0.2	0.3
LOI	13.4	10.7	20.5	0	26.7	16.1	17.8	14.9	16.1	13.9	16	12.5	13.9	21.7	22.6	21.2	21.7

BS: Brandon Shores fly ash, PS: Paul Smith fly ash, DP: Dickerson Precipitator fly ash, L: Lime kiln dust (LKD), LOI: Loss of ignition, Silica ratio=$SiO_2/(Al_2O_3 + Fe_2O_3)$, LSF (Lime saturation factor) =$CaO/(2.8\ SiO_2+1.2Al_2O_3+0.65Fe_2O_3)$, Alumina ratio=Al_2O_3/Fe_2O_3

TABLE 6. Effect of freezing and thawing cycles on summary resilient moduli.

Fly Ash Type	Fly Ash Content (%)	LKD Content (%)	SM_R (Mpa)				Water Content (%)			
Number of Freeze and Thaw Cycles			**0**	**4**	**8**	**12**	**0**	**4**	**8**	**12**
Brandon Shores	10	2.5	228	307	155	103	9	9	11	17
	20	2.5	157	247	169	95	10	10	14	15
Paul Smith	10	5	350	340	222	165	9	11	14	15
	20	5	278	245	105	93	13	13	16	22
Dickerson Precipitator	10	2.5	180	166	144	117	11	11	14	12
	10	5	217	218	158	152	11	10	18	15

LKD: Lime kiln dust

TABLE 7. Required base thickness for different mixture designs for two traffic and excellent drainage conditions (all thickness values are in mm).

Soil or Fly Ash Type	Fly Ash Content (%)	LKD Content (%)	Based on CBR		Based on M_R	
			Case I	Case II	Case I	Case II
Brandon Shores	10	2.5	212	474	205	459
	10	5	176	395	192	431
	20	2.5	219	491	289	647
	20	5	198	445	176	395
Paul Smith	10	2.5	219	491	205	459
	10	5	176	395	159	356
	20	2.5	227	508	235	527
	20	5	227	508	176	395
Dickerson Precipitator	10	2.5	219	491	265	594
	10	5	205	459	167	374
	20	2.5	223	501	227	508
	20	5	212	474	167	374
BRG	0	0	382	846	335	750
GAB	0	0	301	678	212	475
URM	0	0	397	890	353	791

BS: Brandon Shores fly ash, PS: Paul Smith fly ash, DP: Dickerson Precipitator fly ash, LKD: Lime kiln dust, BRG: Bank run gravel, GAB: Graded aggregate base, URM: Unpaved road gravel. The numbers that follow the fly ashes and LKD indicate the percentages by weight of admixtures added to the soil. Minimum thickness requirement (AASHTO Guide 1993) for ESALs greater than 5,000,000 is 152.4 mm.

TABLE 8. Cost analysis for all mixture designs under excellent drainage conditions

FlyAsh Type	Fly Ash Content (%)	Lime Kiln Dust Content (%)	Thickness of the Base Layer (mm)		Cost of Base Materials (x1000$)		Cost of LKD (x1000$)		Cost of Fly Ash (x1000$)		Total Cost of Construction (x1000$)	
			Case I	Case II	Case I	Case II	Case I	Case II	Case I	Case II	Case I	Case II
Brandon Shores	10	2.5	187	419	102.2	228.9	15.5	34.7	7.2	16.2	124.5	388.8
	10	5	182	407	101.9	228.1	30.0	67.3	5.6	12.6	137.5	433.0
	20	2.5	265	593	123.6	276.7	21.1	47.4	17.8	39.9	162.5	486.6
	20	5	159	356	69.3	155.2	24.6	55.0	11.5	25.7	105.3	315.6
Paul Smith	10	2.5	193	432	102.2	228.8	15.5	34.7	16.3	36.5	134.0	397.5
	10	5	167	375	92.1	206.2	27.2	60.8	11.4	25.6	130.1	397.8
	20	2.5	227	509	100.8	225.8	17.3	38.7	32.7	73.2	150.8	415.3
	20	5	177	396	75.2	168.5	26.6	59.7	28.0	62.8	130.0	358.1
Dickerson Precipitator	10	2.5	179	400	96.2	215.5	14.6	32.7	8.2	18.2	119.0	367.1
	10	5	167	375	95	212.8	28.0	62.8	6.2	14.0	129.3	404.9
	20	2.5	193	432	87.9	196.9	15.1	33.7	15.1	33.8	118.1	348.7
	20	5	177	396	78.9	176.9	28.0	62.6	15.6	34.9	122.5	362.0
BRG	0	0	353	791	230.6	516.3	0	0	0	0	230.5	746.7
GAB	0	0	318	712	233.3	522.5	0	0	0	0	233.3	755.8
URM	0	0	398	890	252.4	565.3	0	0	0	0	252.2	565.4

Note: Material cost includes only the material purchase, transportation, fuel and hauling costs.

FIGURES

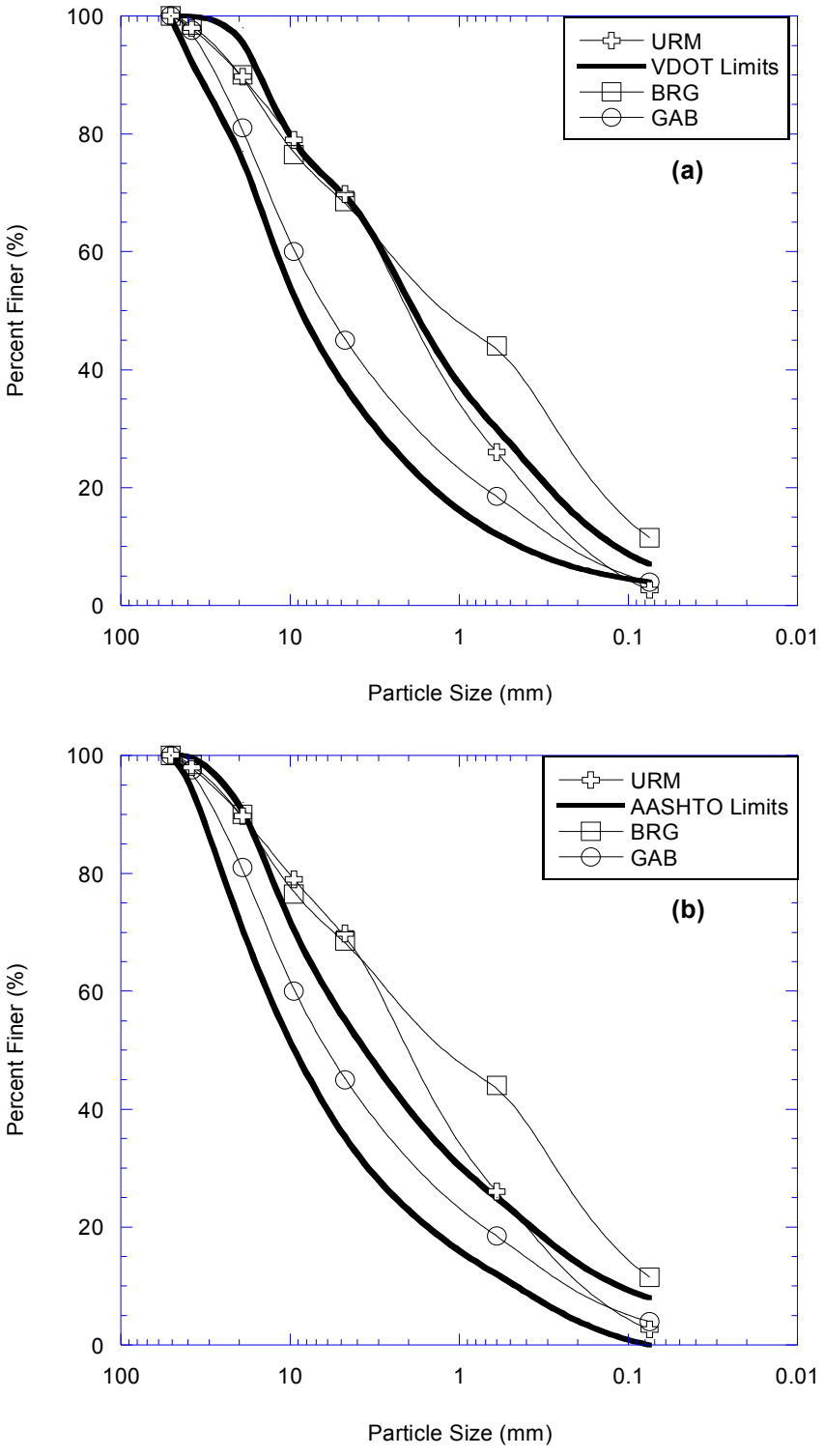

FIGURE 1. Comparison of unpaved road material and the two materials used in base construction in Maryland to (a) VDOT base materials specification, and (b) AASHTO specification. Note: URM: Unpaved road material, BRG : Bank Run Gravel, GAB: Graded aggregate base.

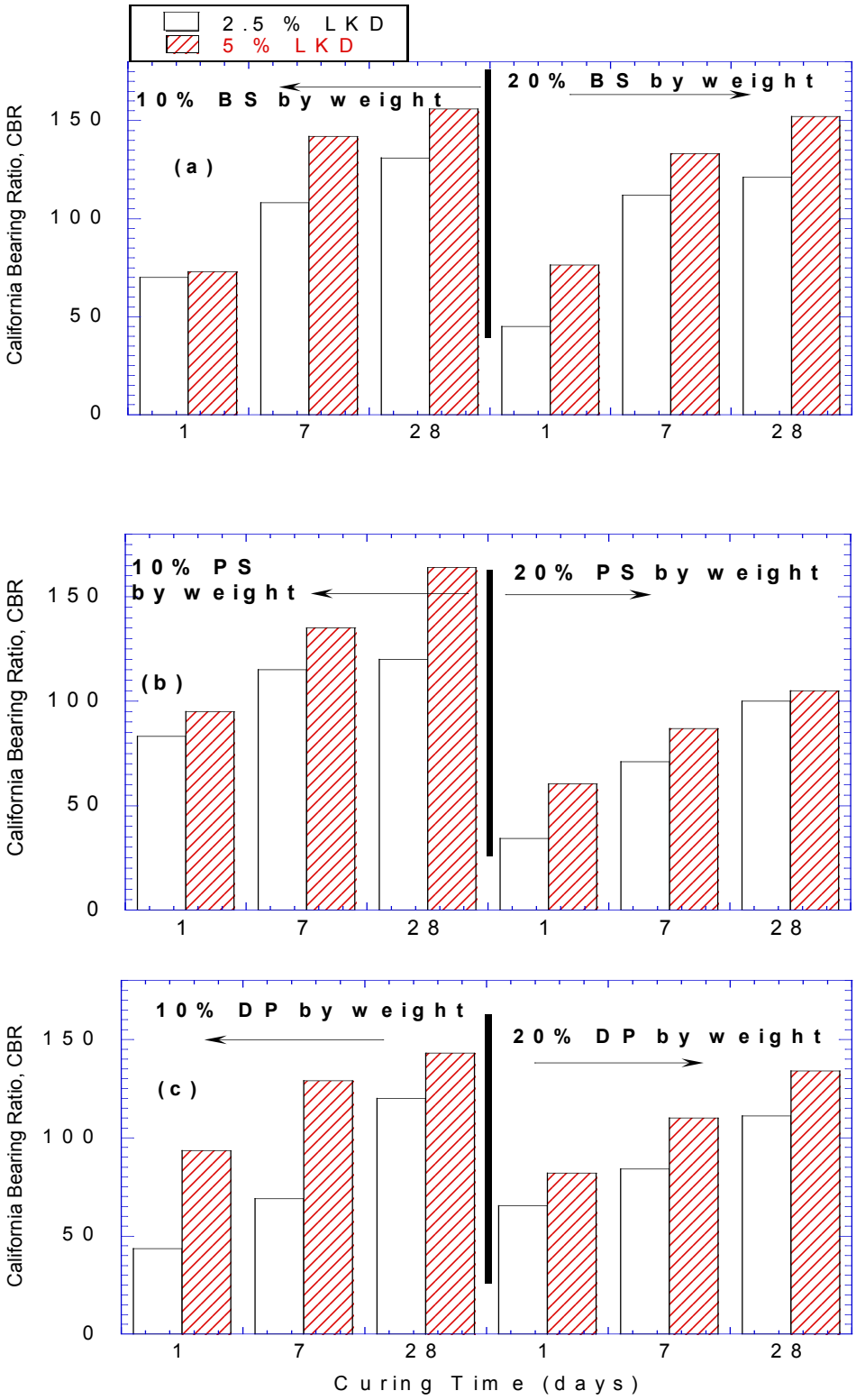

FIGURE 2. Effect of curing time on CBR of mixtures prepared with (a) Brandon Shores fly ash, (b) Paul Smith fly ash, and (c) Dickerson Precipitator fly ash.

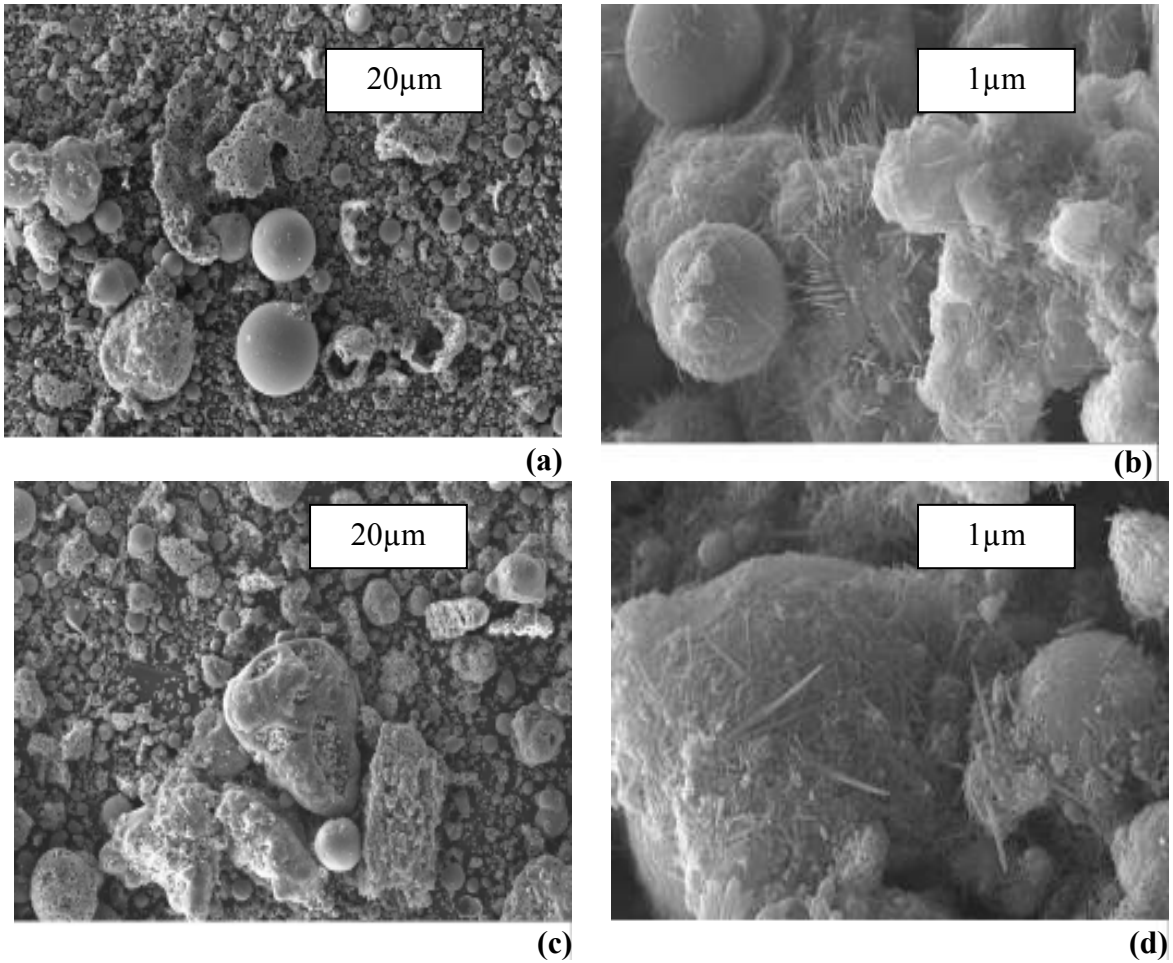

FIGURE 3. SEM photograph of (a) Brandon Shores fly ash, (b) unpaved road material amended with 10% Brandon Shores fly ash and 2.5% LKD by weight (10BS+2.5LKD), (c) Dickerson Precipitator fly ash, and (d) unpaved road material amended with 20% Dickerson Precipitator fly ash and 5% LKD by weight (20DP+5LKD). All specimens were cured for 7 days. LKD: Lime kiln dust.

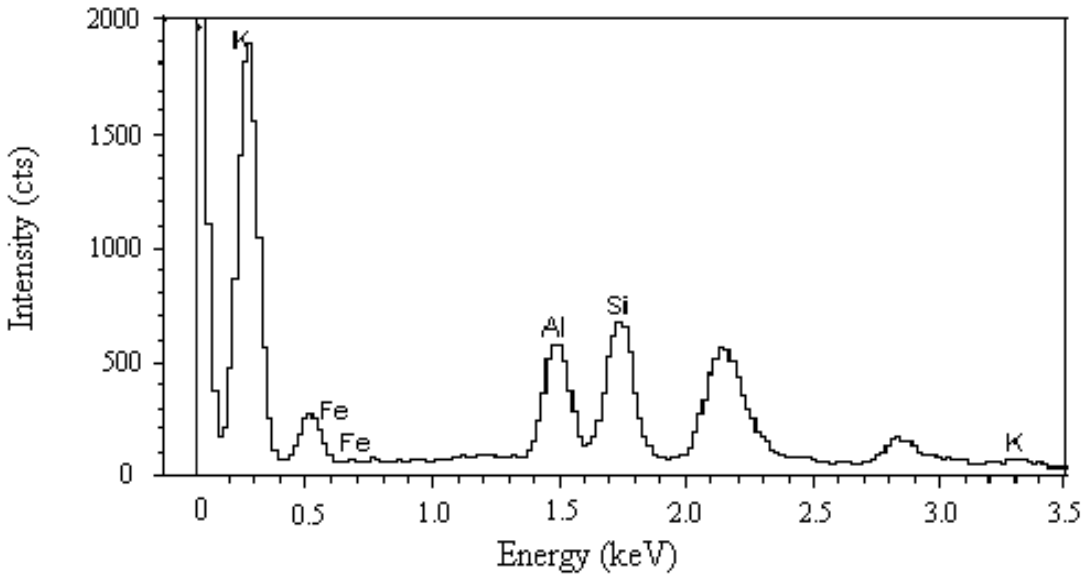

(a)

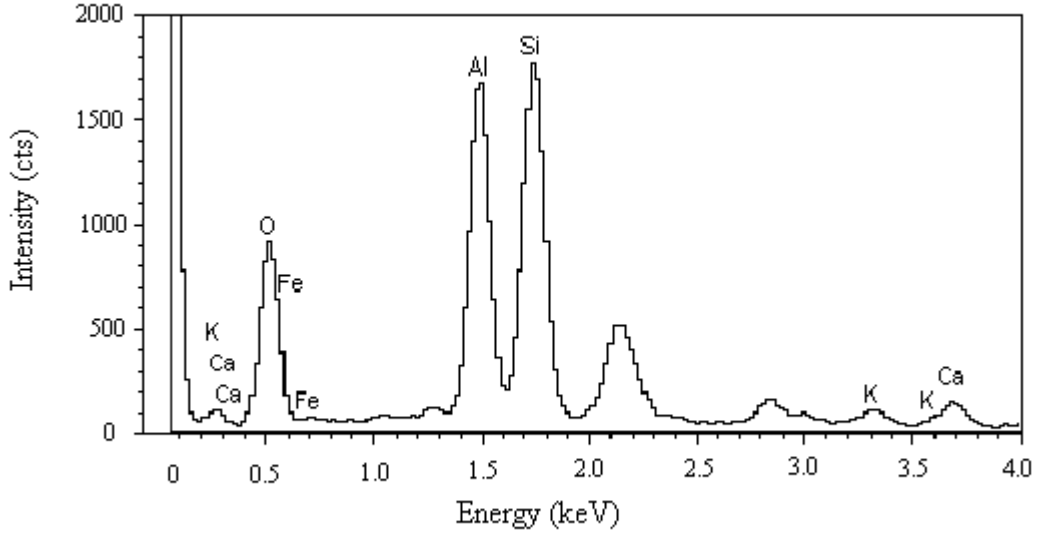

(b)

FIGURE 4. EDX plot of the SEM photograph of (a) Dickerson Precipitator fly ash, and (b) 7-day cured unpaved road material amended with 20% Dickerson Precipitator fly ash and 5% LKD by weight (20DP+5LKD).

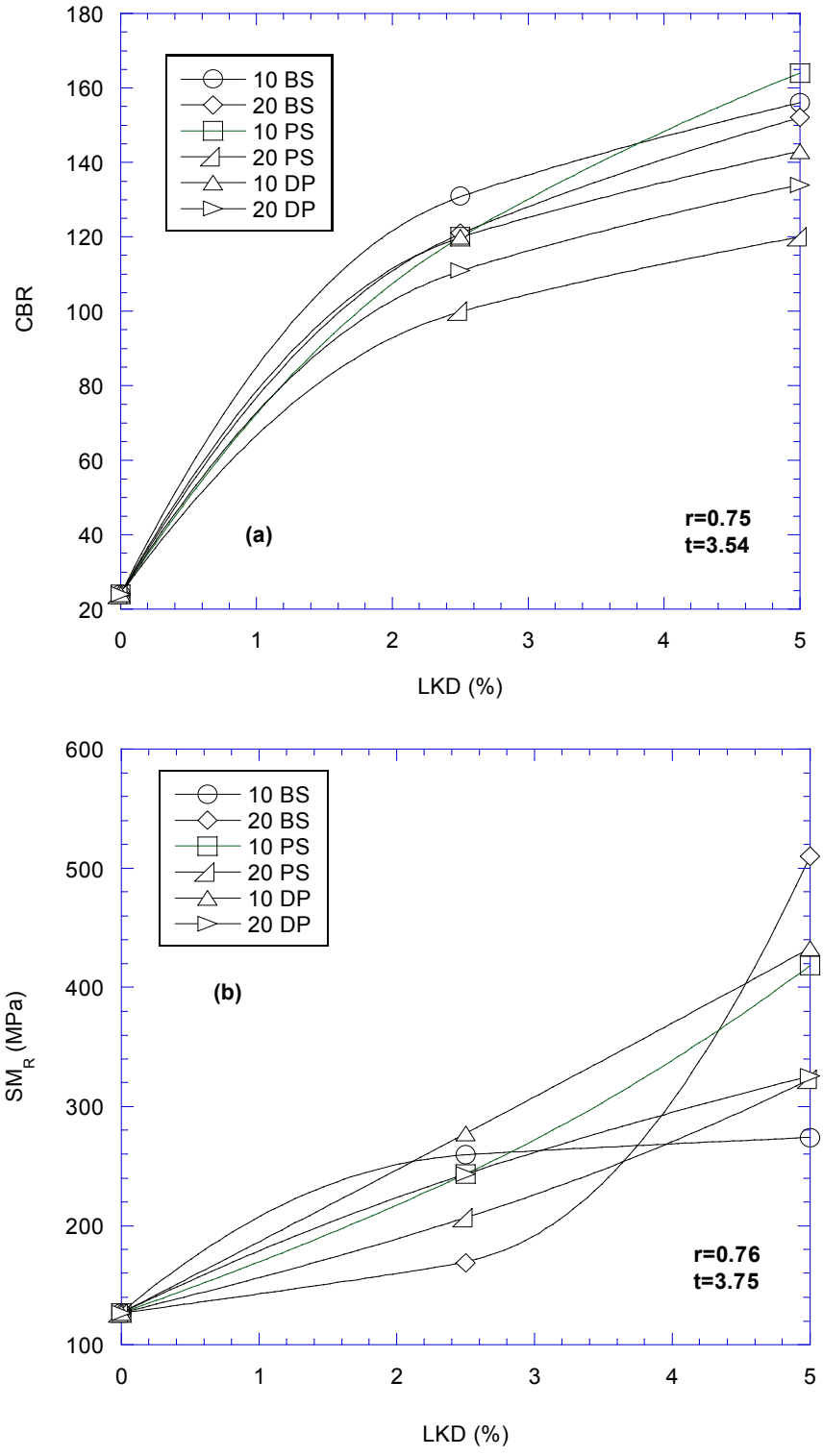

FIGURE 5. Effect of LKD contents on (a) CBR and (b) SM_R of 28-day cured specimens (Note: 10 BS, 20 BS, 10 PS, 20 PS, 10 DP, and 20 DP designate the specimens with 10% and 20% Brandon Shores, Paul Smith, and Dickerson Precipitator fly ash respectively. LKD: Lime Kiln Dust).

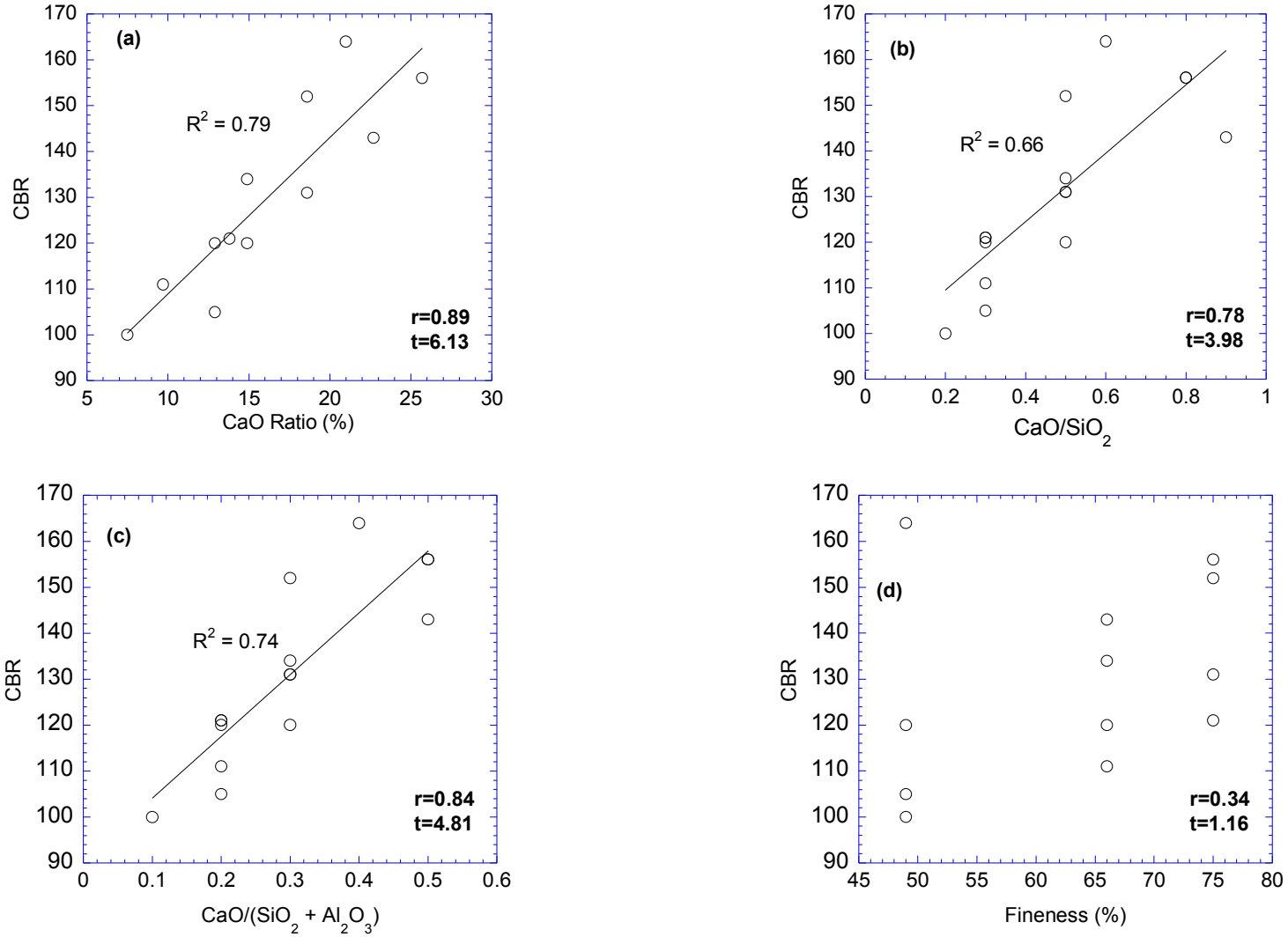

FIGURE 6. Effect of (a) CaO content, (b) CaO/SiO_2, (c) $CaO/(SiO_2 + Al_2O_3)$, and (d) fineness on CBR.

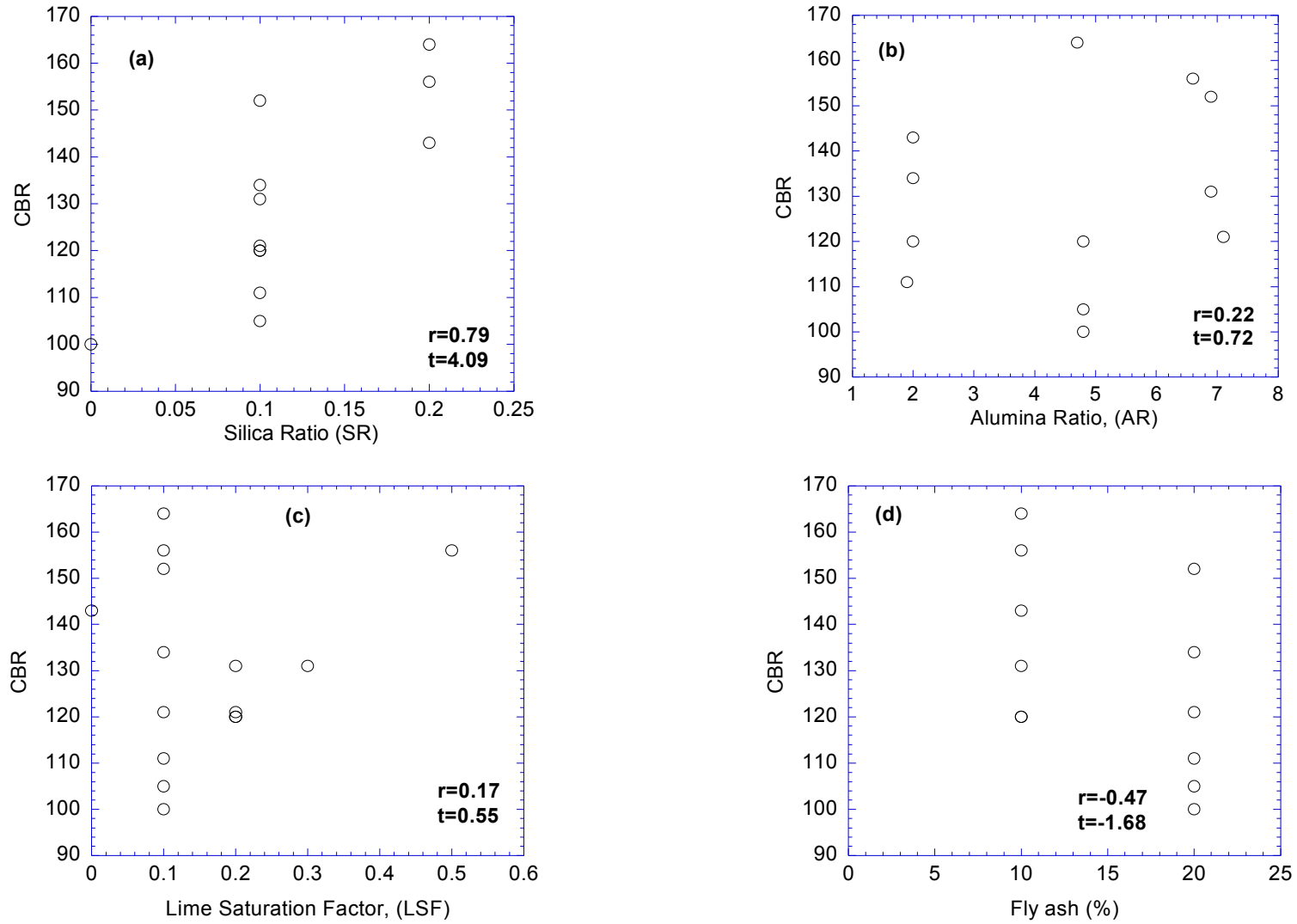

FIGURE 7. Effect of (a) Silica ratio, (b) alumina ratio, (c) lime saturation factor, and (d) fly ash percentage on CBR.

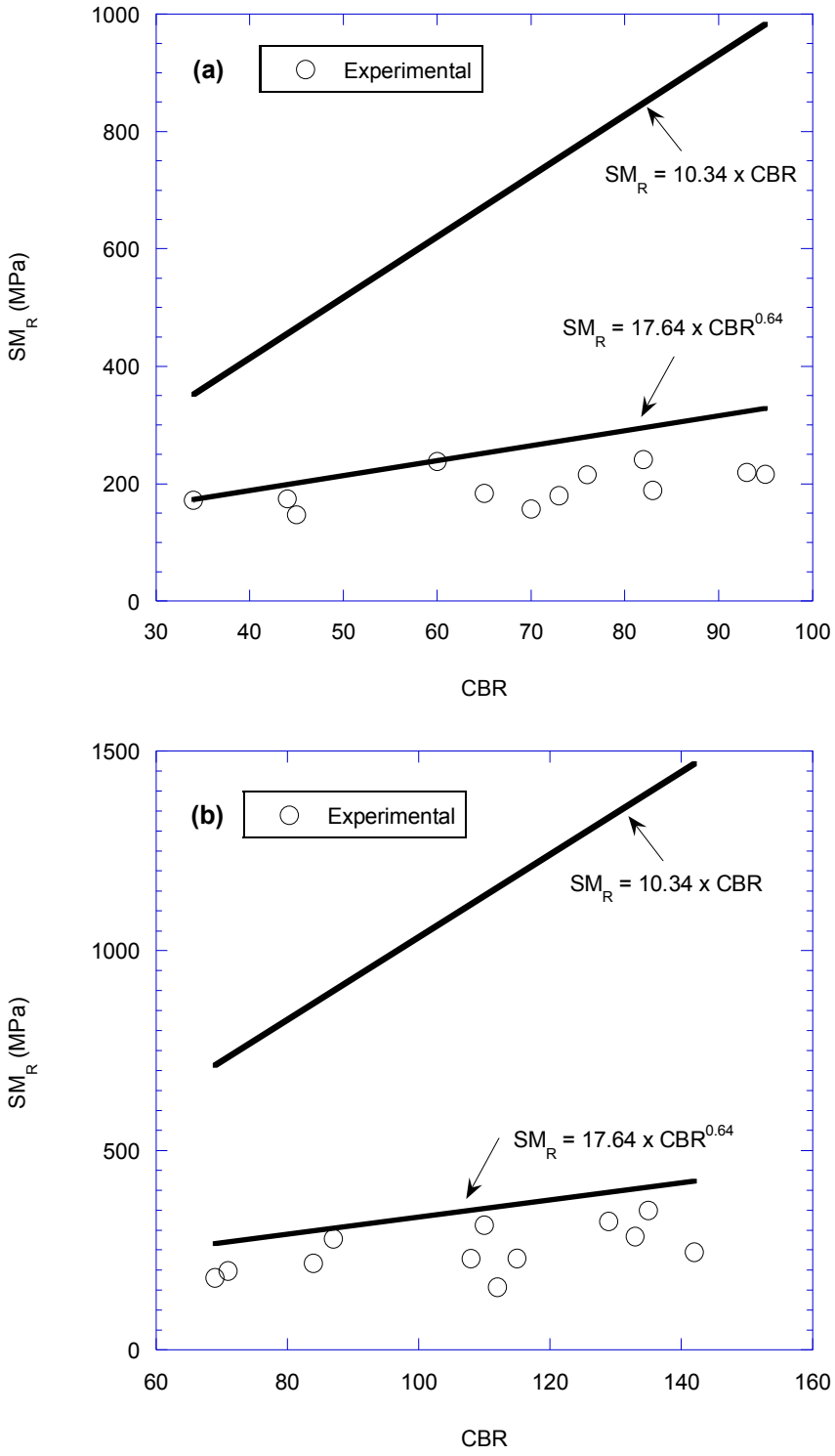

FIGURE 8. CBR versus measured and predicted SM_R for (a) 1 day cured specimens, and (b) 7 days cured specimens

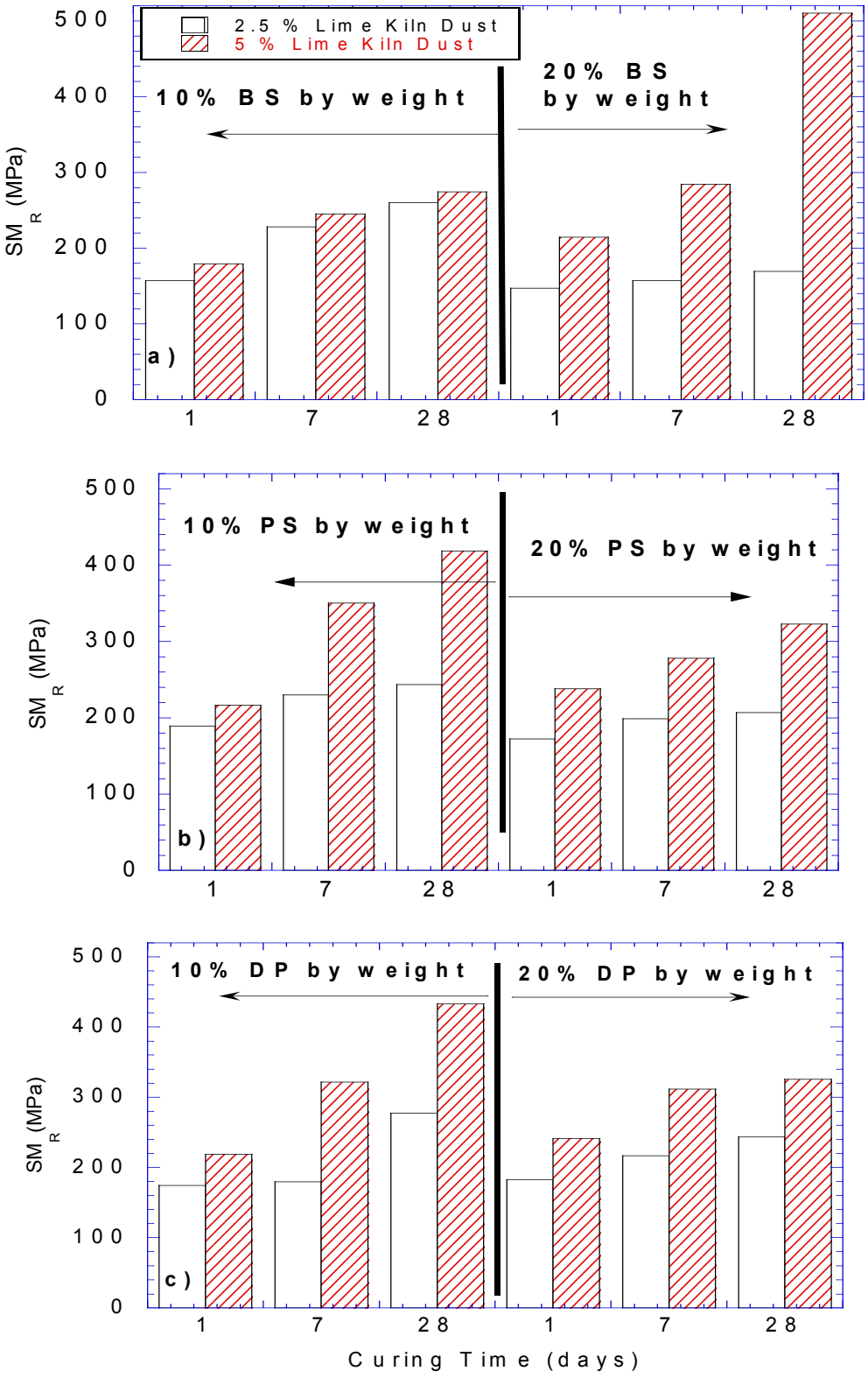

FIGURE 9. Effect of curing time on SM_R of mixtures prepared with (a) Brandon Shores fly ash, (b) Paul Smith fly ash, and (c) Dickerson Precipitator fly ash.

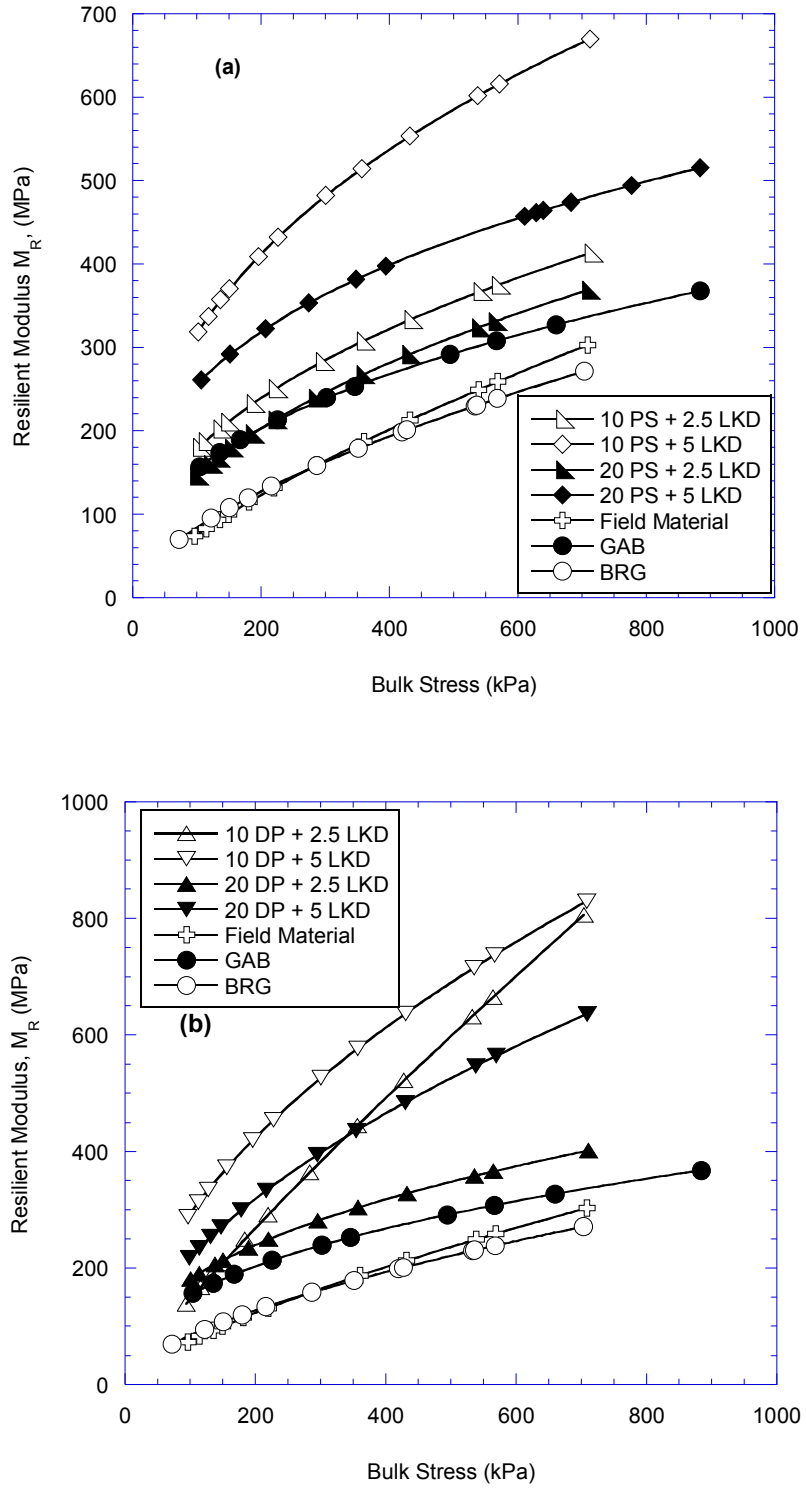

FIGURE 10. Resilient modulus of the 28-day cured specimens with varying bulk stresses: Mixtures prepared with (a) Paul Smith fly ash, and (b) Dickerson Precipitator fly ash

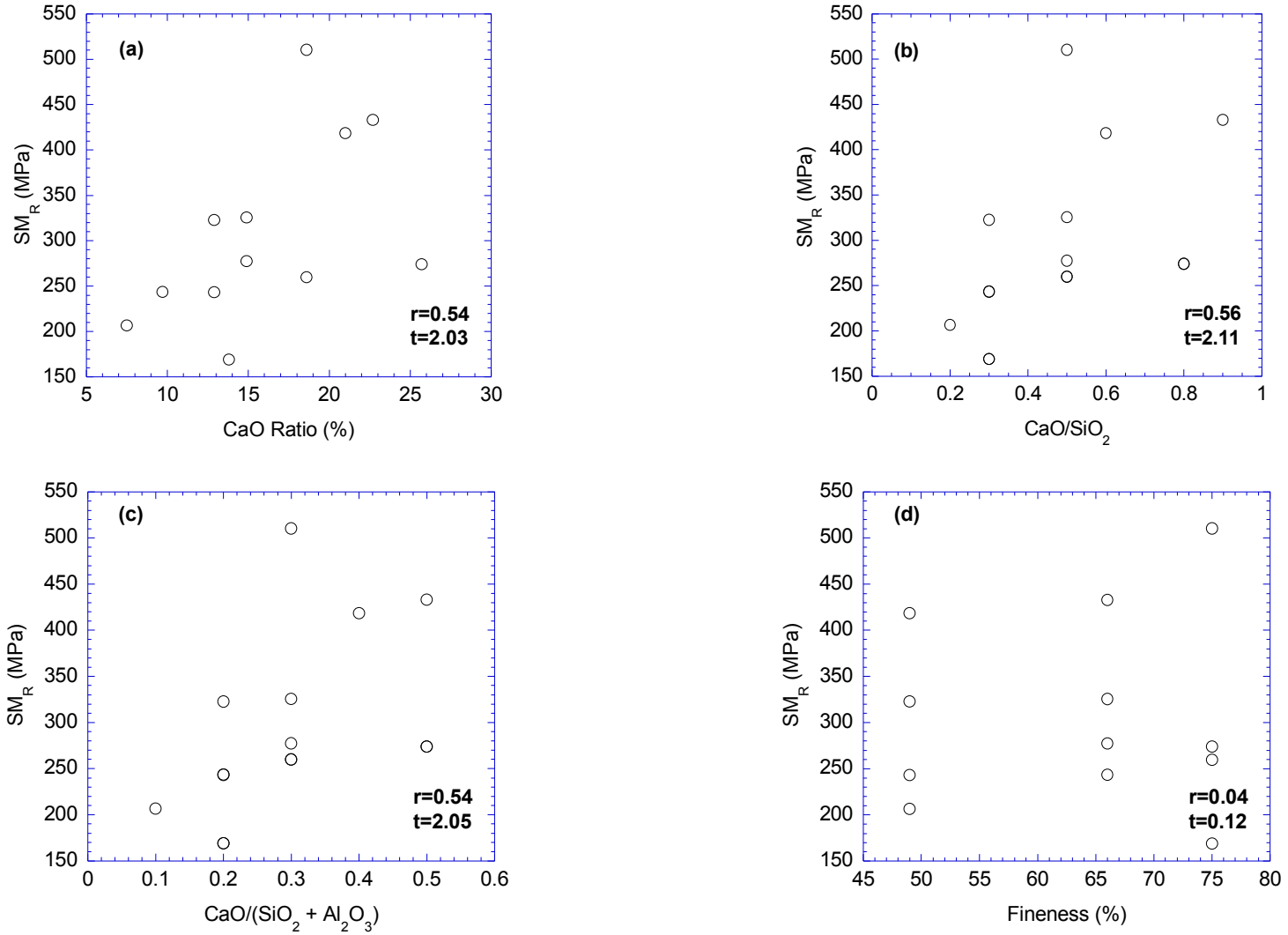

FIGURE 11. Effect of (a) CaO content, (b) CaO/SiO_2, (c) $CaO/(SiO_2 + Al_2O_3)$, and (d) fineness on SM_R.

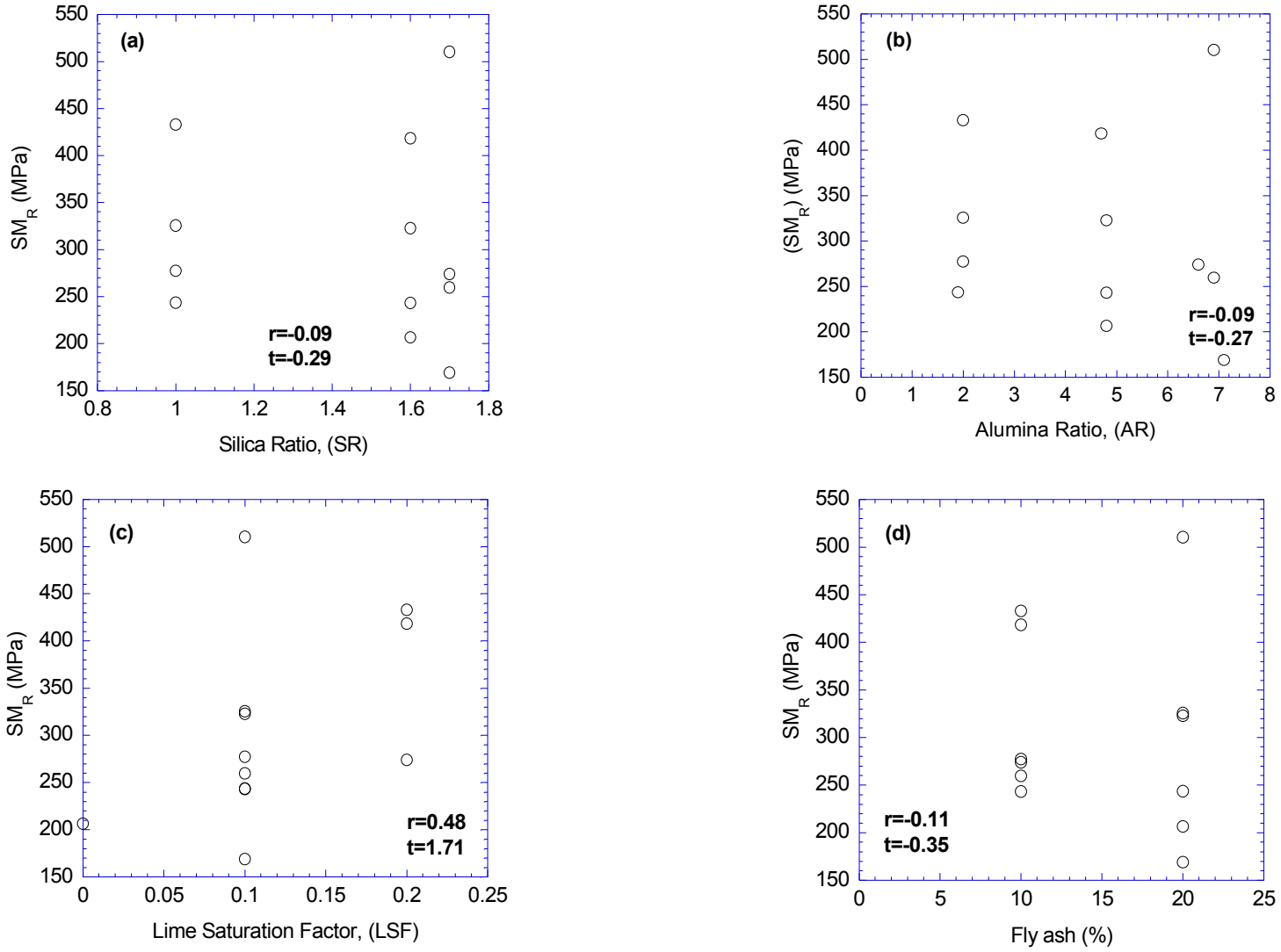

FIGURE 12. Effect of (a) Silica ratio, (b) alumina ratio, (c) LSF , and (d) fly ash percentage on SM_R.

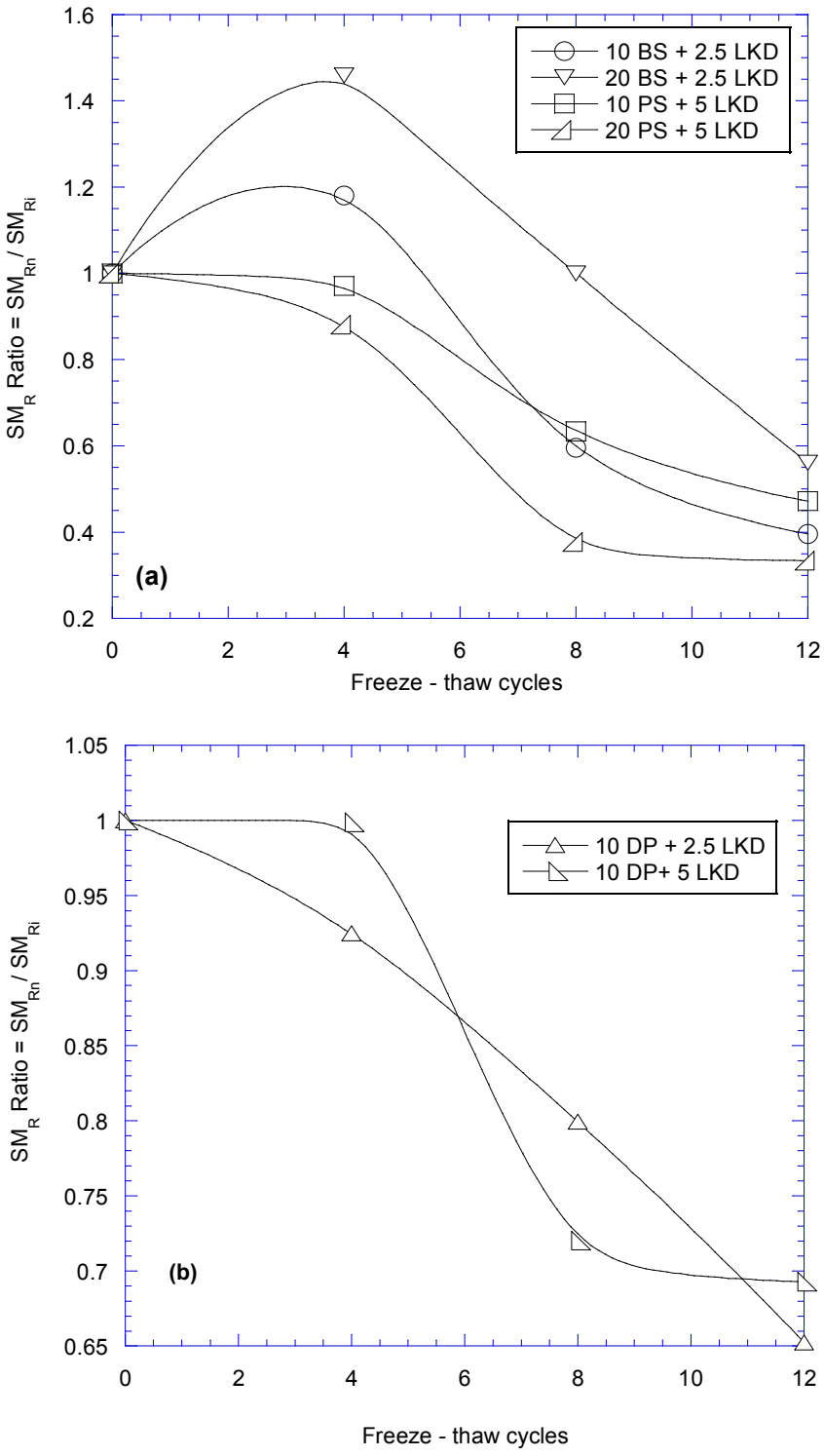

FIGURE 13. Effect of freeze and thaw cycles on SM_R values (Note: 10 BS, 20 BS, 10 PS, 20 PS, 10 DP, and 20 DP designate the specimens with 10% and 20% Brandon Shores, Paul Smith, and Dickerson Precipitator fly ash respectively. LKD: Lime Kiln Dust).

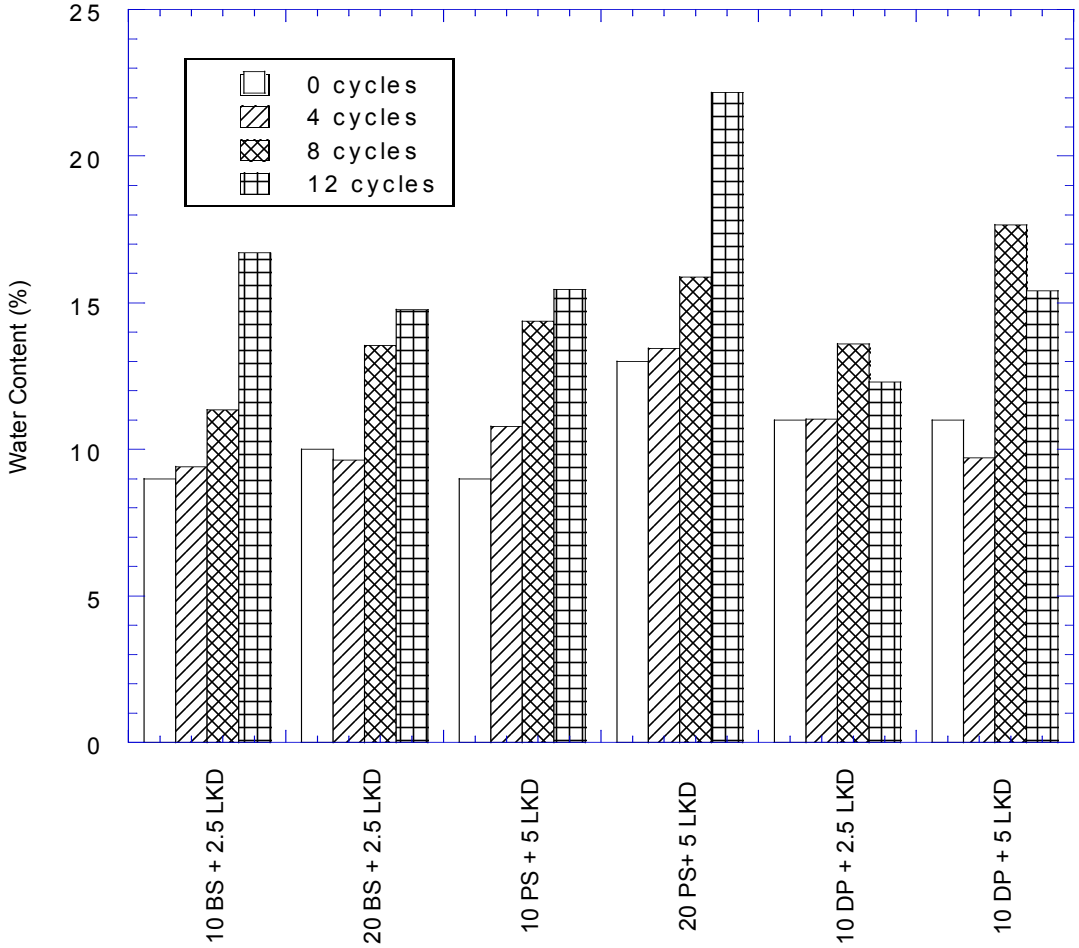

FIGURE 14. Effects of freeze and thaw cycles on water contents (Note: 10 BS, 20 BS, 10 PS, 20 PS, 10 DP, and 20 DP designate the specimens with 10% and 20% Brandon Shores, Paul Smith, and Dickerson Precipitator fly ash respectively. LKD: Lime Kiln Dust).

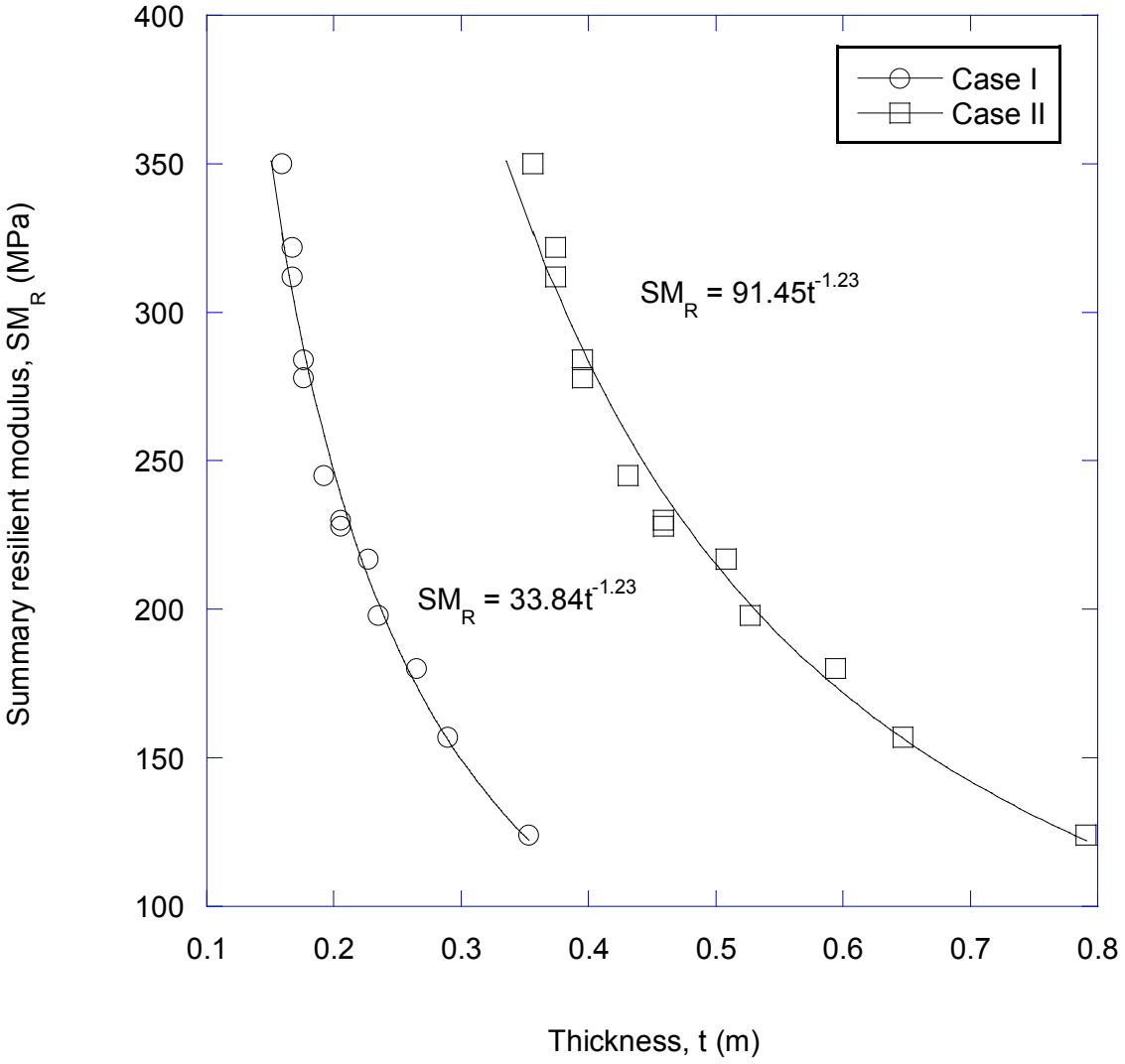

FIGURE 15. Summary resilient modulus as a function of base layer thickness.

APPENDIX

APPENDIX A

CHEMICAL AND PHYSICAL PROPERTIES OF FLY ASHES USED IN THE CURRENT STUDY

Table A.1 Properties of Maryland fly ashes with ASTM C 618 chemical and physical criteria for Class C and Class F fly ash.

Chemical Requirements	**ASTM Requirements**		**BS**	**DP**	**PS**
	Class F	**Class C**			
$SiO_2 + Al_2O_3 + Fe_2O_3$, min (%)	70	50	71.4	71.9	83.2
SO_3, max (%)	5	5	-	-	-
Moisture Content (as-received), max (%)	3	3	1.8	7.7	3.5
Loss on Ignition, max (%)	6	6	13.4	20.5	10.7

Physical Requirements	**ASTM Requirements**		**BS**	**DP**	**PS**
	Class F	**Class C**			
Fineness, max (%)	34	34	25	34	51
Strength Activity @ 7 Days, min (%)	75	75	-	-	-
Strength Activity @ 28 Days, min (%)	75	75	-	-	-
Water Requirement, max (%)	115	115	-	-	-
Autoclave Expansion, max (%)	0.8	0.8	-	-	-
Density Variation, max (%)	5	5	-	-	-
Variation of % Retained on 45-μm filter, max (%)	5	5	-	-	-

A 1. STATISTICAL ANALYSIS

The relationship between CBR or resilient modulus and each of the fly ash chemical characteristics was tested for statistical significance by determining whether the Pearson correlation coefficient between CBR or resilient modulus and each of the fly ash variables is statistically different from zero. For this statistical analysis, the t-statistic (t) is computed from the correlation coefficient (r) as:

$$t = \frac{r - \rho}{\sqrt{\frac{1 - r^2}{n - 2}}}$$

where ρ is the population correlation coefficient (assumed to be zero) and n is the number of degrees of freedom (24 for CBR test data and 20 for resilient modulus test data in this analysis). A comparison then is made between t and the critical t (t_{cr}) corresponding to a significance level α. If $t > t_{cr}$, then the Pearson correlation coefficient is significantly different from zero and a significant relationship exists between CBR or resilient modulus and the fly ash property. In this analysis, α was set at 0.05 (the commonly accepted significance level), which corresponds to $t_{cr} = 2.06$ for CBR test results and $t_{cr}=2.09$ for resilient modulus test results.

APPENDIX B

BASE COURSE TESTING PROTOCOL

B.1 COMPACTION CURVES FOR ALL SPECIMENS

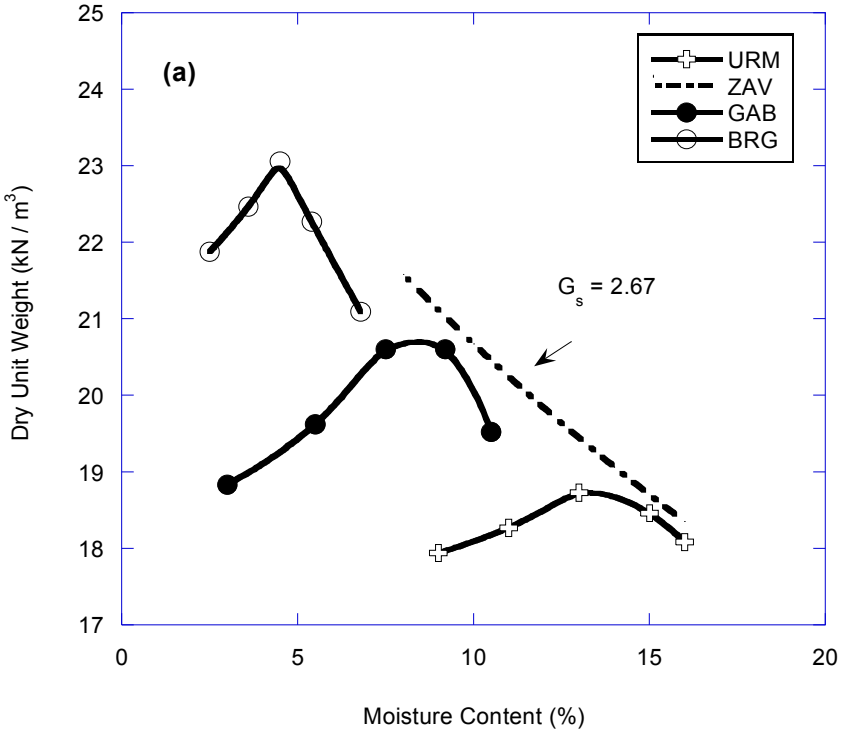

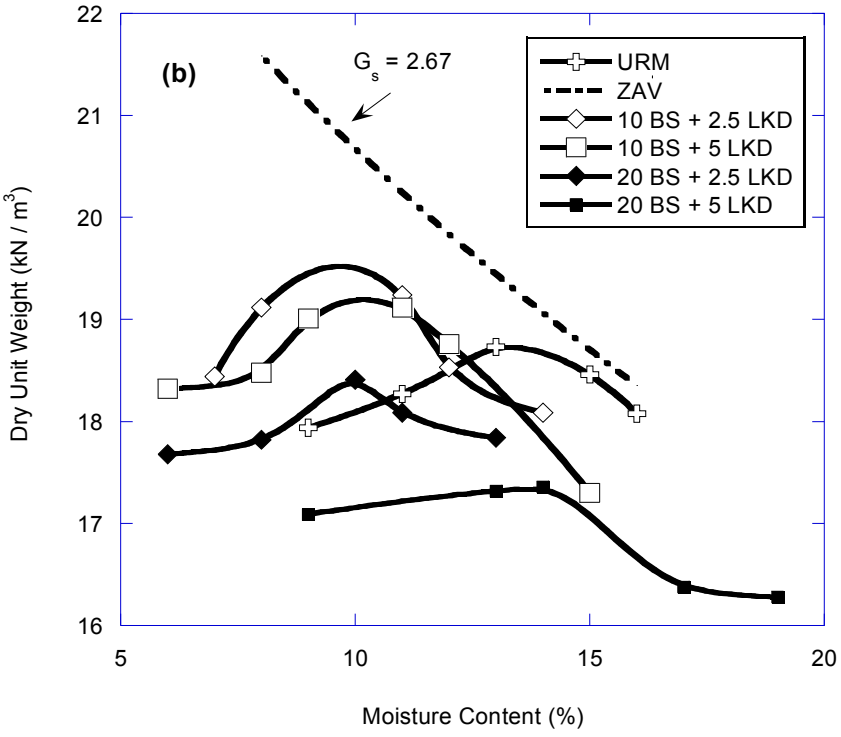

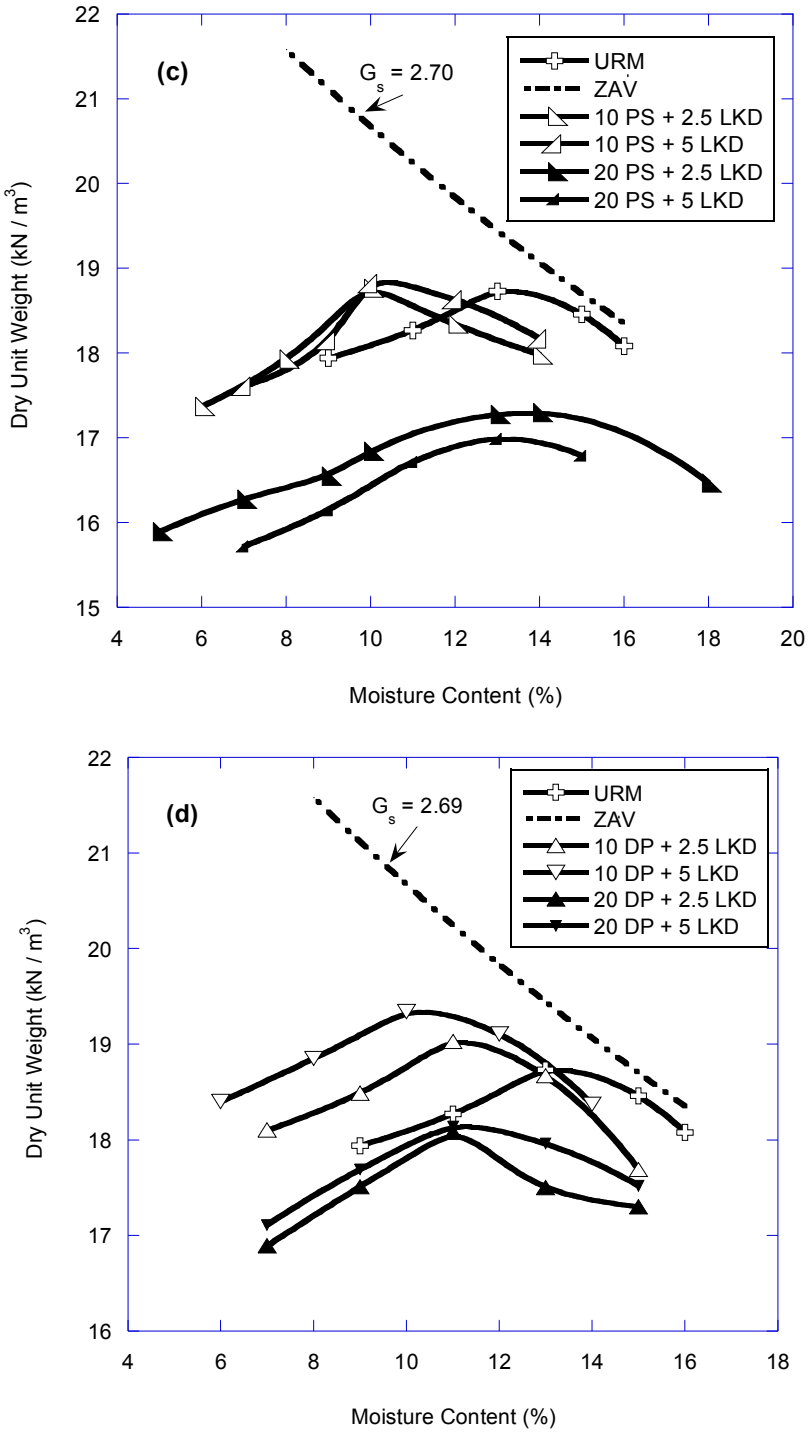

Figure B. 1 Compaction curves for (a) conventional base materials, (b) mixtures prepared with Brandon Shores fly ash, (c) mixtures prepared with Paul Smith fly ash, and (d). mixtures prepared with Dickerson Precipitator fly ash (Note: 10 BS, 20 BS, 10 PS, 20 PS, 10 DP, and 20 DP designate the specimens with 10% and 20% Brandon Shores, Paul Smith, and Dickerson Precipitator fly ash respectively. LKD: Lime Kiln Dust, GAB: Graded Aggregate Base, RGB: Bank Run Gravel).

B.2 RESILIENT MODULUS TEST PROTOCOL AND LOADING SEQUENCE SUMMARY TABLE

The resilient modulus test procedure was based on the AASHTO T 307-99 a protocol for testing base and highway base and subbase materials. The specimens of 101.6 mm in diameter and 230.2 mm in height were compacted in split molds at their OMC in eight layers using the standard Proctor energy. The deformation was measured externally with two spring-loaded linear variable differential transducers (LVDT). A Geocomp LoadTrac-II loading frame and associated hydraulic power unit system was used to load the specimens. Conditioning stress was 103 kPa. Confining stress was kept between 20.7 and 138 kPa during loading stages, and the deviator stress was increased from 20.7 kPa to 276 kPa and applied 100 repetitions at each step. The loading sequence, confining pressure, and data acquisition were controlled by a personal computer equipped with RM 5.0 software. The base and subbase testing sequence is shown in Table B.1

The resilient modulus of soil was computed by using the common model defined by Moosazadh and Witczak (1981). A summary resilient modulus (SM_R) was computed at a bulk stress of 208 kPa, following the suggestions provided in NCHRP 1-28A.

Table B.1 AASHTO T 307-99 resilient modulus testing sequence for base and subbase materials.

Sequence No.	Confining Pressure, S_3 (kPa)	Maximum Axial Stress, S_{max} (kPa)	Cyclic Stress, S_{cyclic} (kPa)	Constant Stress, 0.1 S_{max} (kPa)	Cycles
0	103.4	103.4	93.1	10.3	500
1	20.7	20.7	18.6	2.1	100
2	20.7	41.4	37.3	4.1	100
3	20.7	62.1	55.9	6.2	100
4	34.5	34.5	31	3.5	100
5	34.5	68.9	62	6.9	100
6	34.5	103.4	93.1	10.3	100
7	68.9	68.9	62	6.9	100
8	68.9	137.9	124.1	13.8	100
9	68.9	206.8	186.1	20.7	100
10	103.4	68.9	62	6.9	100
11	103.4	103.4	93.1	10.3	100
12	103.4	206.8	186.1	20.7	100
13	137.9	103.4	93.1	10.3	100
14	137.9	137.9	124.1	13.8	100
15	137.9	275.8	248.2	27.6	100

B.3 STEP-BY-STEP RESILIENT MODULUS TEST PROCEDURE

1) Turn on Geocomp Load Trac II

2) Turn the air pressure pump on

3) Measure the specimen height and diameter

4) Place the porous stone on bottom plate

5) Place the filter paper on bottom porous stone

6) Place the specimen on bottom plate

7) Place the filter paper on top of the specimen

8) Place the porous stone on filter paper

9) Place the top plate on top of the specimen

10) Place rubber membrane over specimen using a mold

11) Place two O- rings on both bottom and top of the plates to hold the membrane in place

12) Plug the drainage tubes on top plate.

13) Place the cell on bottom cap

14) Place cover plate, it should not be tight

15) Place LVDT on top of chamber

16) Screw cover plate with three rods carefully

17) Plug air supply hose into cell

18) Log into PC and open the Resilient modulus RM version 5.0 software

19) Input Specimen height, diameter, and weight.

20) Input the loading and pressure data which is designed for base and subbase test protocol

21) Click on the load calibration menu and check the applied load with the load data that you entered

22) Click run test and save the file.

B.4 RESILIENT MODULUS TEST APPARATUS

Figure B.2 Photo of Resilient Modulus Testing Equipment

B.5 PHOTOS OF SOIL SAMPLES

Figure B.3. GAB (a), URM (b), and BRG (c)

(Note: GAB: Graded aggregate Base, URM: Unpaved road material, BRG: Bank run gravel.)

APPENDIX C

CBR AND RESILIENT MODULUS TEST RESULTS

C1. CBR VERSUS MEASURED SM_R

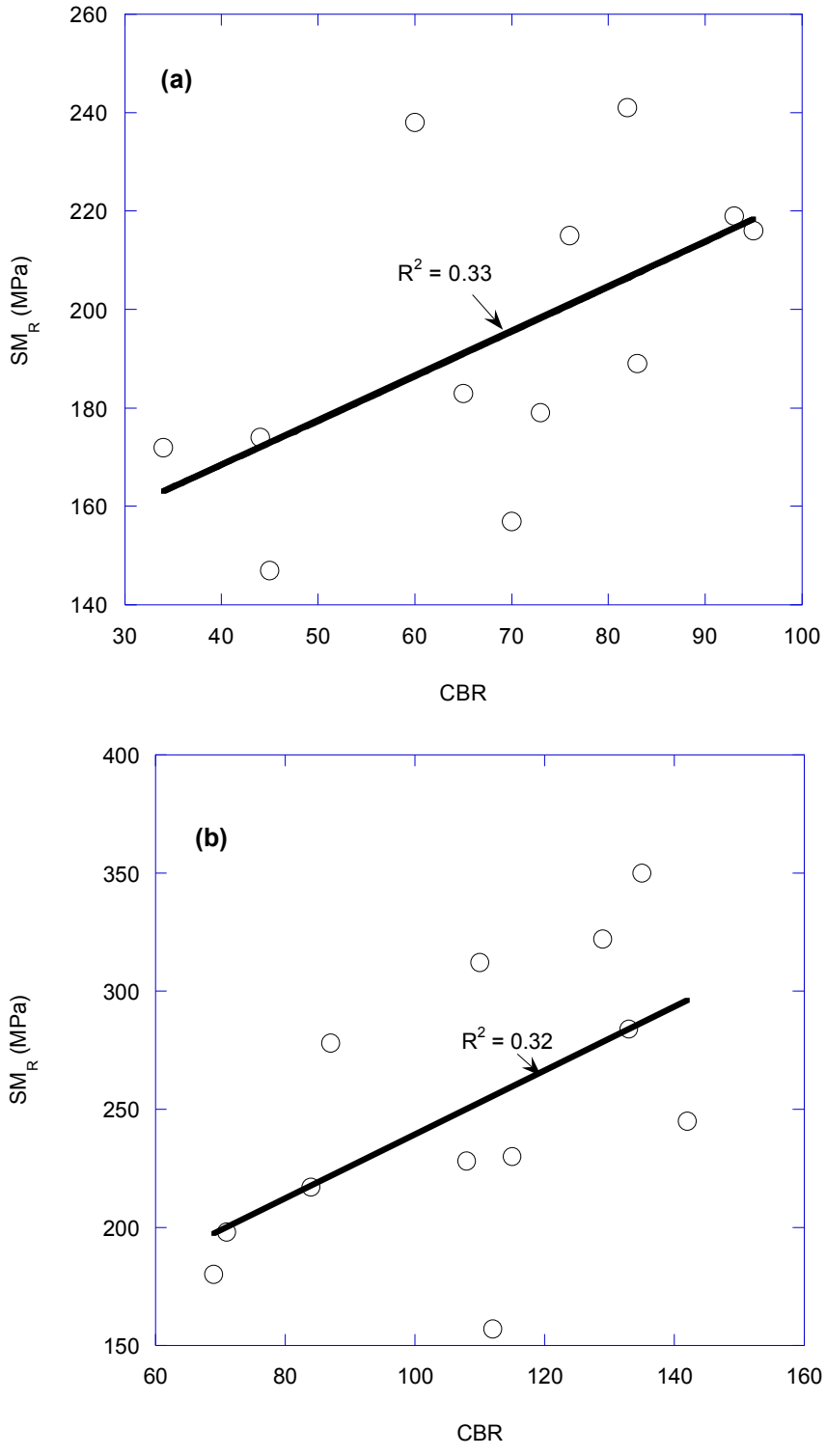

Figure C.1. CBR versus measured SM_R vs. CBR graph for (a)1 day cured specimens, and (b) 7 days cured specimens.

C2. CBR VERSUS PREDICTED SM_R

Table C.1. Predicted SM_R values based on CBR values

Fly Ash Type	Fly Ash Content (%)	Lime Kiln Dust Content (%)	CBR		SM_R (Mpa) ($SM_R = 10.34 \times CBR$)		SM_R (Mpa) ($SM_R = (17.64 \times CBR^{0.64})$)	
			1 Day Cured	7 Days Cured	1 Day Cured	7 Days Cured	1 Day Cured	7 Days Cured
Brandon Shores	10	3	70	108	724	1117	267	353
	10	5	73	142	755	1468	275	420
	20	3	45	112	465	1158	201	361
	20	5	76	133	786	1375	282	403
Paul Smith	10	3	83	115	858	1189	298	367
	10	5	95	135	982	1396	325	407
	20	3	34	71	352	734	168	270
	20	5	60	87	620	900	242	307
Dickerson Precipitator	10	3	44	69	455	713	199	265
	10	5	93	129	962	1334	321	395
	20	3	65	84	672	869	255	300
	20	5	82	110	848	1137	296	357
GAB	0	0	42		434		193	
BRG	0	0	27		279		145	
URM	0	0	24		248		135	

APPENDIX D

BASE THICKNESS CALCULATIONS FOR SPECIMENS SUBJECTED TO FREEZE-THAW

D.1 BASE THICKNESS CALCULATIONS FOR SPECIMENS SUBJECTED TO FREEZE-THAW

Table D.1. Base thickness values based on SM_R values for traffic case I (all thickness values are in mm)

Specimen Name	Base thickness values based on SM_R values			
	Cycle Number			
	0	4	8	12
10 BS + 2.5 LKD	205	318	530	530
20 BS + 2.5 LKD	289	265	530	530
10 PS + 5 LKD	159	223	289	289
20 PS + 5 LKD	176	454	454	578
10 DP + 2.5 LKD	265	318	318	454
10 DP + 5 LKD	167	289	289	302

Table D.2. Base thickness values based on SM_R values for traffic case II (all thickness values are in mm)

Specimen Name	Base Thickness values based on SM_R values			
	Cycle Number			
	0	4	8	12
10 BS + 2.5 LKD	459	712	1186	1186
20 BS + 2.5 LKD	647	593	1186	1186
10 PS + 5 LKD	356	501	647	647
20 PS + 5 LKD	395	1017	1017	1294
10 DP + 2.5 LKD	593	712	712	1017
10 DP + 5 LKD	374	647	647	678

BS: Brandon Shores fly ash, PS: Paul Smith fly ash, DP: Dickerson Precipitator fly ash, LKD: Lime kiln dust. The numbers that follow the fly ashes and LKD indicate the percentages by weight of admixtures added to the soil. Minimum thickness requirement (AASHTO Guide 1993) for ESALs greater than 5,000,000 is 152.4 mm.

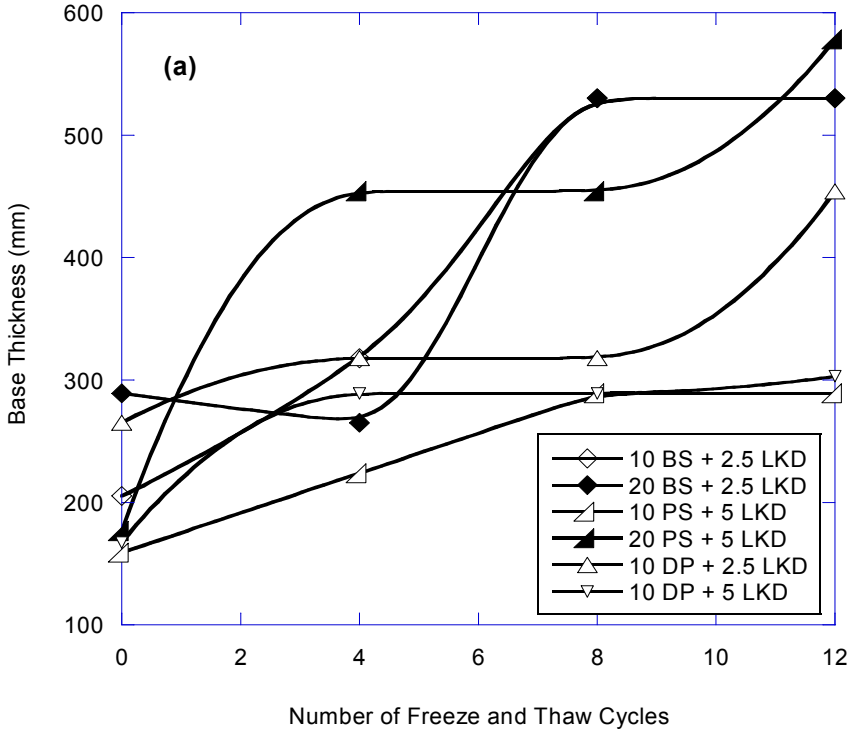

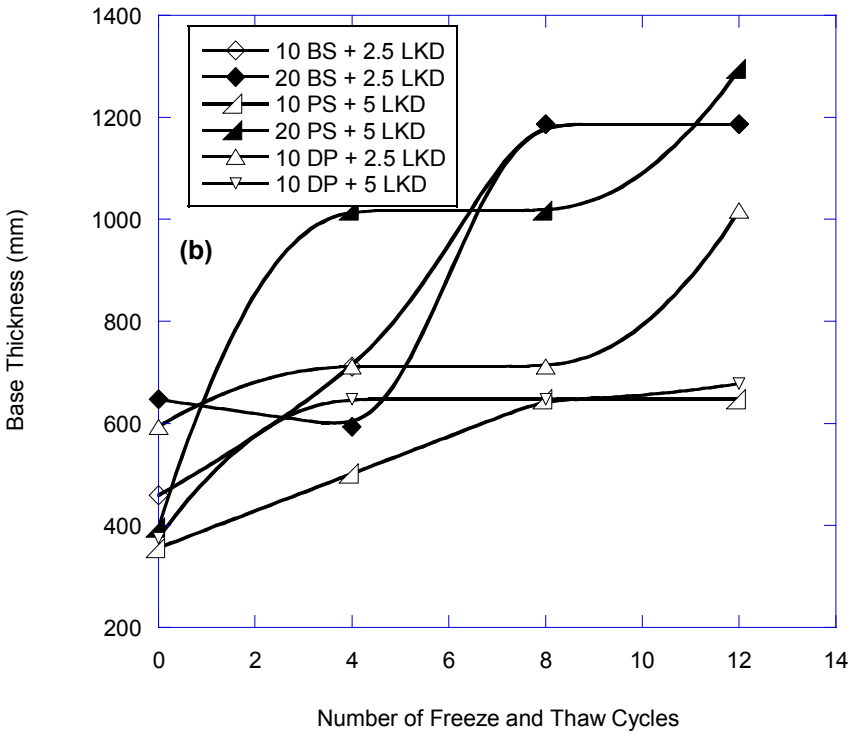

Figure D.1 Required thickness vs. number of freeze and thaw cycles (a) for traffic case I, and (b) for traffic case II

APPENDIX E

BASE THICKNESS AND COST CALCULATIONS FOR SPECIMENS UNDER DIFFERENT DRAINAGE CONDITIONS

E.1 BASE THICKNESS CALCULATIONS FOR SPECIMENS UNDER DIFFERENT DRAINAGE CONDITIONS

Table E1. Required base thickness for different mixture designs for two traffic conditions under good drainage conditions (all thickness values are in mm).

Fly Ash Type	Fly Ash Content (%)	Lime Kiln Dust Content (%)	Thickness of the Base Layer Based on CBR		Thickness of the Base Layer Based on SM_R	
			Case I	Case II	Case I	Case II
Brandon Shores	10	2.5	277	555	277	555
	10	5	262	524	269	539
	20	2.5	314	629	392	787
	20	5	262	524	235	472
Paul Smith	10	2.5	314	629	285	572
	10	5	262	524	248	497
	20	2.5	336	674	336	674
	20	5	332	665	262	524
Dickerson Precipitator	10	2.5	314	629	265	530
	10	5	269	539	248	497
	20	2.5	327	656	285	572
	20	5	277	555	262	524
BRG	0	0	523	1049	589	1180
GAB	0	0	428	858	471	944
URM	0	0	673	1349	589	1180

Table E2. Required base thickness for different mixture designs for two traffic conditions under fair drainage conditions (all thickness values are in mm).

Fly Ash Type	Fly Ash Content (%)	Lime Kiln Dust Content (%)	Thickness of the Base Layer Based on CBR		Thickness of the Base Layer Based on SM_R	
			Case I	Case II	Case I	Case II
Brandon Shores	10	2.5	412	760	412	760
	10	5	389	718	400	738
	20	2.5	467	861	584	1076
	20	5	389	718	350	646
Paul Smith	10	2.5	467	861	424	783
	10	5	389	718	369	680
	20	2.5	500	923	500	923
	20	5	493	910	389	718
Dickerson Precipitator	10	2.5	467	861	393	726
	10	5	400	738	369	680
	20	2.5	486	897	424	783
	20	5	412	760	389	718
BRG	0	0	778	1435	875	1614
GAB	0	0	637	1174	700	1292
URM	0	0	1000	1845	875	1614

Table E3. Required base thickness for different mixture designs for two traffic conditions under poor drainage conditions (all thickness values are in mm).

Fly Ash Type	Fly Ash Content (%)	Lime Kiln Dust Content (%)	Thickness of the Base Layer Based on CBR		Thickness of the Base Layer Based on SM_R	
			Case I	Case II	Case I	Case II
Brandon Shores	10	2.5	637	1101	637	1101
	10	5	601	1039	619	1069
	20	2.5	722	1247	902	1559
	20	5	601	1039	541	935
Paul Smith	10	2.5	722	1247	656	1134
	10	5	601	1039	570	985
	20	2.5	773	1336	773	1336
	20	5	762	1318	601	1039
Dickerson Precipitator	10	2.5	722	1247	608	1051
	10	5	619	1069	570	985
	20	2.5	752	1299	656	1134
	20	5	637	1101	601	1039
BRG	0	0	1203	2079	1353	2339
GAB	0	0	984	1701	1083	1871
URM	0	0	1547	2673	1353	2339

Table E4. Cost Analysis for different mixture designs for two traffic conditions under good drainage conditions (all thickness values are in mm).

Fly Ash Type	Fly Ash Content (%)	Lime Kiln Dust Content (%)	Thickness of the Base Layer (mm)		Cost of Base Materials (x1000$)		Cost of LKD (x1000$)		Cost of Fly Ash (x1000$)		Total Cost of Construction (x1000$)	
			Case I	Case II	Case I	Case II	Case I	Case II	Case I	Case II	Case I	Case II
Brandon Shores	10	2.5	277	555	151.3	303.3	229.6	46.0	10.7	21.5	185.0	534.4
	10	5	269	539	150.8	302.4	445.0	89.2	8.3	16.7	203.7	595.2
	20	2.5	392	787	183.0	366.7	313.4	62.8	26.4	52.9	240.7	670.3
	20	5	235	472	102.7	205.8	363.4	72.8	17.0	34.1	156.0	434.6
Paul Smith	10	2.5	285	572	151.3	303.2	229.5	46.0	24.2	48.4	198.4	547.6
	10	5	248	497	136.4	273.4	402.3	80.6	16.9	33.9	193.5	547.5
	20	2.5	336	674	149.3	299.3	255.8	51.3	48.4	97.1	223.3	573.9
	20	5	262	524	111.4	223.4	394.5	79.1	41.5	83.1	192.4	494.8
Dickerson Precipitator	10	2.5	265	530	142.5	285.6	216.1	43.3	12.0	24.1	176.1	505.0
	10	5	248	497	140.7	282.1	415.1	83.2	9.30	18.5	191.5	556.8
	20	2.5	285	572	130.2	261.0	223.0	44.7	22.3	44.8	174.8	480.5
	20	5	262	524	117.0	234.4	414.0	83.0	23.1	46.2	181.4	498.8
BRG	0	0	523	1049	341.4	684.4	0	0	0	0	341.4	102.6
GAB	0	0	471	944	345.5	692.5	0	0	0	0	345.5	103.8
URM	0	0	589	1180	373.8	749.4	0	0	0	0	373.8	749.4

Table E5. Cost Analysis for different mixture designs for two traffic conditions under fair drainage conditions (all thickness values are in mm).

Fly Ash Type	Fly Ash Content (%)	Lime Kiln Dust Content (%)	Thickness of the Base Layer (mm)		Cost of Base Materials (x1000$)		Cost of LKD (x1000$)		Cost of Fly Ash (x1000$)		Total Cost of Construction (x1000$)	
			Case I	Case II	Case I	Case II	Case I	Case II	Case I	Case II	Case I	Case II
Brandon Shores	10	2.5	412	760	225.0	303.3	34.2	63.0	16.0	29.4	275.2	641.5
	10	5	389	738	218.1	302.4	64.3	122.1	12.0	22.8	294.4	718.8
	20	2.5	467	1076	217.7	366.8	37.3	86.0	31.4	72.3	286.3	739.0
	20	5	389	646	169.6	205.8	60.0	99.7	28.1	46.6	257.7	563.1
Paul Smith	10	2.5	467	783	247.5	303.2	37.6	63.0	39.5	66.2	324.5	690.7
	10	5	389	680	214.1	273.4	63.2	110.3	26.6	46.4	303.8	687.5
	20	2.5	500	923	222.1	299.3	38.0	70.2	72.0	132.8	332.1	701.6
	20	5	493	718	210.1	223.4	74.4	108.2	78.2	113.8	362.6	694.2
Dickerson Precipitator	10	2.5	467	726	251.4	285.6	38.2	59.3	21.2	33.0	310.8	655.7
	10	5	400	680	227.2	282.1	67.0	113.9	14.9	25.4	309.1	705.1
	20	2.5	486	783	221.8	261.0	38.0	61.2	38.1	61.3	297.9	620.0
	20	5	412	718	184.1	234.4	65.2	113.6	36.3	63.2	285.6	633.5
BRG	0	0	778	1435	507.7	684.4	0	0	0	0	507.7	1192.1
GAB	0	0	637	1292	467.1	692.5	0	0	0	0	467.1	1159.6
URM	0	0	1000	1614	635.4	749.4	0	0	0	0	635.3	749.4

Table E6. Cost Analysis for different mixture designs for two traffic conditions under poor drainage conditions (all thickness values are in mm).

Fly Ash Type	Fly Ash Content (%)	Lime Kiln Dust Content (%)	Thickness of the Base Layer (mm)		Cost of Base Materials ($)		Cost of LKD ($)		Cost of Fly Ash ($)		Total Cost of Construction ($)	
			Case I	Case II	Case I	Case II	Case I	Case II	Case I	Case II	Case I	Case II
Brandon Shores	10	2.5	637	1101	347.9	601.3	52.8	91.2	24.7	42.7	425.360	1117.8
	10	5	619	1069	346.8	599.3	102.3	176.8	19.1	33.1	468.184	1244.3
	20	2.5	902	1559	420.6	726.9	72.1	124.5	60.6	104.8	553.300	1404.7
	20	5	541	935	236.0	407.8	83.5	144.4	39.1	67.5	358.566	910.8
Paul Smith	10	2.5	656	1134	347.8	601.0	52.8	91.2	55.5	95.9	456.056	1148.3
	10	5	570	985	313.5	541.8	92.5	159.8	38.9	67.3	444.906	1146.6
	20	2.5	773	1336	343.3	593.3	58.8	101.6	111.3	192.4	513.416	1208.3
	20	5	601	1039	256.2	442.7	90.7	156.7	95.4	164.9	442.247	1041.7
Dickerson Precipitator	10	2.5	608	1051	327.5	566.0	49.7	85.9	27.7	47.8	404.890	1056.8
	10	5	570	985	323.5	559.1	95.4	164.9	21.3	36.7	440.203	1164.2
	20	2.5	656	1134	299.3	517.2	51.3	88.6	51.4	88.8	401.939	1007.8
	20	5	601	1039	268.8	464.6	95.2	164.5	53.0	91.6	416.995	1046.1
BRG	0	0	1203	2079	784.9	1356.5	0	0	0	0	784.887	2141.4
GAB	0	0	1083	1871	794.3	1372.7	0	0	0	0	794.246	2166.9
URM	0	0	1353	2339	859.4	1485.2	0	0	0	0	859.415	1485.3

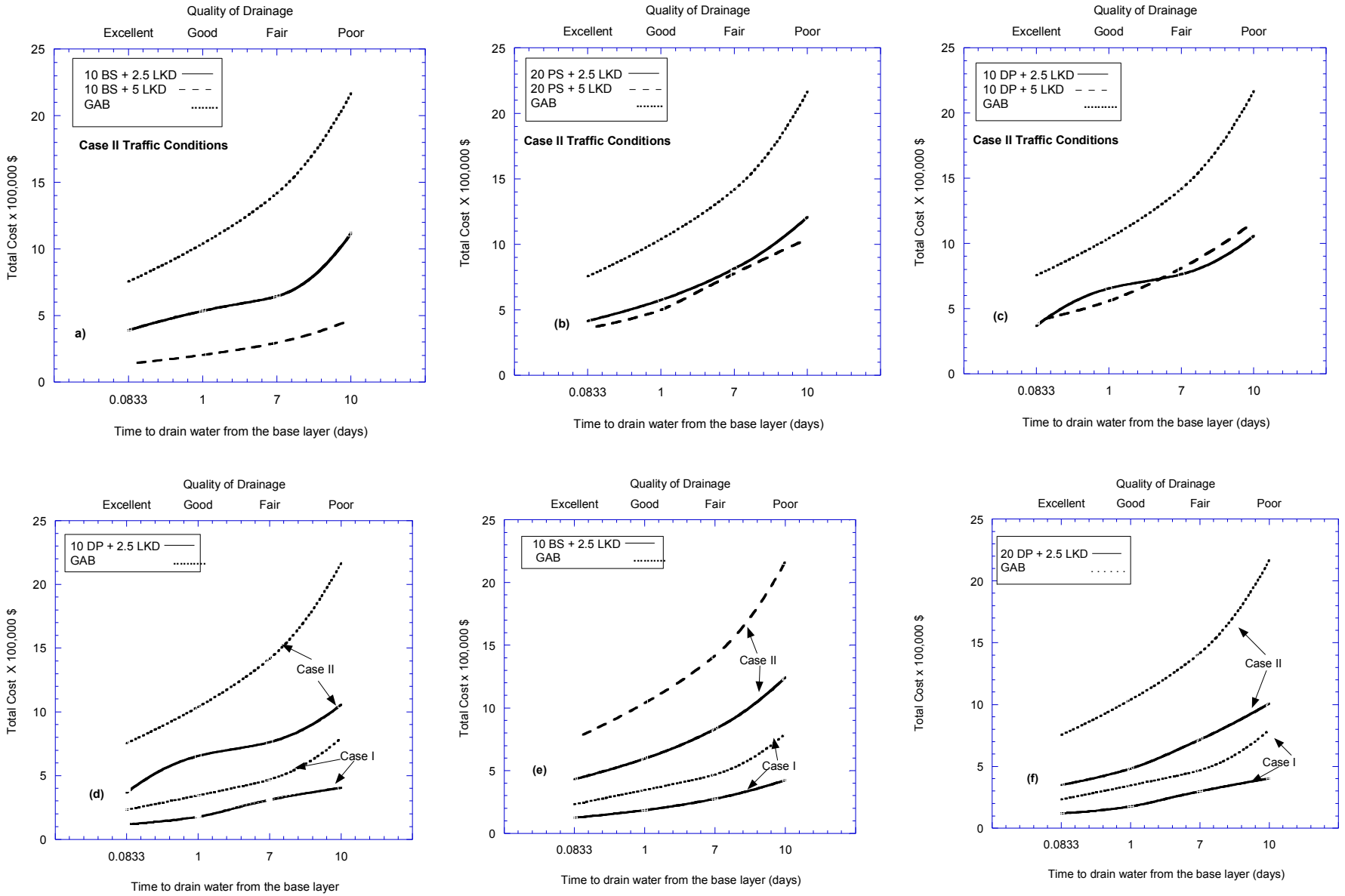

FigureE.1. Effect of LKD addition (a),(b),(c) and traffic conditions(d), (e), (f) on total construction fee of the highway base layer. BS: Brandon Shores fly ash, PS: Paul Smith fly ash, DP: Dickerson Precipitator fly ash, LKD: Lime kiln dust. The numbers that follow the fly ashes and LKD indicate the percentages by weight of admixtures added to the soil.

REFERENCES

AASHTO Guide (1993). "*Guide for Design of Pavement Structures*", American Association of State Highway and Transportation Officials, Washington, D.C.

ACAA (2003). "*2001 Coal Combustion Product Production and Use*", American Coal Ash Association, Denver, Colorado

ARA (2004). "Guide for Mechanistic-Empirical Design on New and Rehabilitated Pavement Structures," NCHRP Project 1-37A. Prepared for National Cooperative Highway Research Program, Washington, D.C.

Arora, S. and Aydilek, A.H. (2005). "Class F Fly Ash Amended Soils as Highway Base Materials", *Journal of Materials in Civil Engineering,* Vol. 17, No. 6, pp. 640-649.

Asphalt Institute (2003). "*Thickness Design –Highways and Streets*", Manual Series, No. 1, Asphalt Institute, Lexington, Kentucky, 110 p.

Bin-Shafique, S., Edil, T., Benson, C., and Senol, A. (2004). "Incorporating a fly ash stabilized layer into pavement design-Case study." *Geotechnical engineering*, Institution of Civil Engineers, London, Vol. 157, No. GE4, 239–249.

Buhler, S.R. and Cerato, A.B. (2007). "Stabilization of Oklahoma Expansive Soils Using Lime and Class C Fly Ash", *ASCE Geotechnical Special Publication,* 162, pp. 1-10.

Camargo, F.F. (2008). "Strength and Stiffness of Recycled Base Materials Blended with Fly Ash", M.S. Thesis, University of Wisconsin-Madison, 123 p.

Conner, J.R. (1990). "*Chemical Fixation and Solidification of Hazardous Wastes*", Van Nostrand Reinfold, New York, 692 p.

Consoli, N. C., Prietto P. D. M., Carraro, J. A. H., and Heineck, K., S. (2001). "Behavior of Compacted Soil-Fly Ash-Carbide Lime Mixtures." *Journal of Geotechnical and Geoenvironmental Engineering*, Vol. 127, No. 9, pp. 774-782.

Cross, S. A. and Young, D. A. (1997). Evaluation of Type C Fly Ash in Cold-in-Place Recycling, *Journal of the Transportation Research Board,* 1583, pp. 82–90.

DiGioia, A. M. and Nuzzo, W. L. (1972). "Fly Ash as Structural Fill," *J. Power Div.,* ASCE, New York, Vol. 98 (1), pp. 77-92.

Edil, T.B., Acosta , A.A., and Benson, C.H. (2006). "Stabilizing Soft Fine-Grained Soils with Fly Ash", *Journal of Materials in Civil Engineering*, Vol. 18, No. 2, pp. 283-294.

Edil, T. B., Benson, C., Bin-Shafique, M., Tanyu, B., Kim, W. and Senol, A. (2002). "Field evaluation of construction alternatives for roadways over soft subgrade", *Journal of the Transportation Research Board,* 1786, pp. 36-48.

Gray, D. H., and Lin, Y. K. (1972). "Engineering Properties of Compacted Fly Ash,"*J. of Soil Mech. and Found. Engrg.*, ASCE, New York, Vol. 98 (4), pp. 361-380.

Guney, Y., Aydilek, A.H., and Demirkan, M.M. (2006). "Geoenvironmental Behavior of Foundry Sand Amended Mixtures for Highway Subbases", *Waste Management,* Vol. 26, pp. 932-945.

Hatipoglu, B., Edil, T., and Benson, C. (2008). "Evaluation of base prepared from road surface gravel stabilized with fly ash", *ASCE Geotechnical Special Publication,* 177, pp. 288-295.

Heukelom, W., and Foster, C. (1960). “Dynamic Testing of Pavements.” *Journal of Soil Mechanics and Foundation Division, Vol.* 86, No. 1, pp.1–28.

Huang, Y. H. (1993). “*Pavement Analysis and Design*”, Prentice-Hall, Inc., New Jersey, 805 p.

Janz, M. and Johansson, S.-E. (2002). "The Function of Different Binding Agents in Deep Stabilization," Report 9. Swedish Deep Stabilization Research Centre, Linkoping, Sweden.

Kumar, A., Walia, B.S., and Bajaj, A.(2007). “Influence of Fly Ash, Lime, and Polyster Fibers on Compaction and Strength Properties of Expansive Soils”, *Journal of Materials in Civil Engineering,* Vol. 19, No. 3, pp. 242-248.

Li, L., Benson, C. H., Edil, T. B., Hatipoglu, B., and Tastan, E. (2007). “Evaluation of recycled asphalt pavement material stabilized with fly ash”, *ASCE Geotechnical Special Publication (CD-ROM)*, 169.

Moosazedh, J., and Witczak, M. (1981). “Prediction of Subgrade Moduli for Soil that Exhibits Nonlinear Behavior”, *Journal of the Transportation Research Board,* 810, pp. 10-17.

PCA (2009). Portland Cement Association, www.cement.org

Powell, W., Potter, J., Mayhew, H., and Nunn, M. (1984). *The Structural* D*esign of Bituminous Roads*, *TRRL Laboratory Report 1132*, Transportation and Road Research Laboratory, Crowthorne, Berkshire, U.K, 62 p.

Rosa, M. (2006). “Effect of Freeze and Thaw Cycling on Soils Stabilized using Fly Ash,” *MS Thesis*, University of Wisconsin-Madison, Madison, WI.

Saylak, D., Mishra, S.K., Mejeoumov, G.G., and Shon, C.C. (2008). "Fly Ash-Calcium Chloride Stabilization in Road Construction", *Proceedings of 87th Annual Meeting (CD ROM)*, Transportation Research Board, Washington, D.C.

Sawangsuriya, A. and Edil, T. B. (2005), "Evaluating stiffness and strength of pavement materials, geotechnical engineering." *Geotechnical Engineering*, Institution of Civil Engineers, London, Vol. 158, No. GE4, 217–230.

Shao, L., Liu, S., Du, Y., Jing, F. and Fang, L. (2008). "Experimental Study on the Stabilization of Organic Clay with Fly Ash and Cement Mixed Method", *ASCE Geotechnical Special Publication,* 179, pp.20-27.

Simonsen, E., Janoo, V., and Isacsson, U. (2002). "Resilient properties of unbound road material during seasonal frost conditions", *Journal of Cold Region Eng.*, 16(1), pp. 28-50.

Tastan, O., Benson, C.H., Edil, T.B., and Aydilek, A.H. (2009). "Stabilization of Organic Soils with Fly Ashes", *Journal of Geotechnical and Geoenvironmental Engineering*, submitted.

Taylor, H.F.W. (1997). "Cement Chemistry", Second edition, Thomas Telford, Inc.

Vishwanathan, R., Saylak, D., and Estakhri, C. (1997). "Stabilization of Subgrade Soils Using Fly Ash", *Proceedings of the Ash Utilization Symposium, CAER*, Kentucky, pp. 204-211.

Wen, H., Baugh, J., and Edil, T. (2007). "Use of Cementitious High Harbon Fly ash to Stabilize Recycled Pavement Materials as Pavement Base Material", *Proceedings of 86th Annual Meeting (CD ROM)*, Transportation Research Board, Washington, D.C.

Wen, H., Warner, J., and Edil, T. (2008). "Laboratory comparison of crushed aggregate and recycled pavement material with and without high-carbon fly ash", *Proceedings of 87th Annual Meeting (DVD)*, Transportation Research Board, Washington, D.C.

Zaman, M., and Naji, K. (2003). "Effect of freeze-thaw cycles on class C fly ash stabilized aggregate base", *Proceedings of 82nd Annual Meeting (CD ROM)*, Transportation Research Board, Washington, D.C.